

# NASA CONTRACTOR REPORT

NASA CR-764

NASA CR-764

GPO PRICE \$ \_\_\_\_\_

CFSTI PRICE(S) \$ \_\_\_\_\_

Hard copy (HC) 3.00

Microfiche (MF) .65

ff 653 July 65

5-31

N 68-28135

FACILITY FORM 602

(ACCESSION NUMBER)	(THRU)
<u>52</u>	<u>1</u>
(PAGES)	(CODE)
(NASA CR OR TMX OR AD NUMBER)	(CATEGORY)
<u>✓</u>	<u>07</u>

## STUDY OF ADVANCED ANTENNA TECHNIQUES FOR RENDEZVOUS RADAR

by B. J. Forman, S. N. Vodopia, and W. H. Kummer

Prepared by  
 HUGHES AIRCRAFT COMPANY  
 Culver City, Calif.  
 for Langley Research Center



STUDY OF ADVANCED ANTENNA TECHNIQUES  
FOR RENDEZVOUS RADAR

By B. J. Forman, S. N. Vodopia, and W. H. Kummer

Distribution of this report is provided in the interest of information exchange. Responsibility for the contents resides in the author or organization that prepared it.

Prepared under Contract No. NAS 1-2621 by  
HUGHES AIRCRAFT COMPANY  
Culver City, Calif.

for Langley Research Center

NATIONAL AERONAUTICS AND SPACE ADMINISTRATION



PRECEDING PAGE BLANK NOT FILMED.

CONTENTS

	Page
I. INTRODUCTION . . . . .	1
II. SUMMARY OF ANTENNA SYSTEM CONSIDERATIONS AND REQUIREMENTS . . . . .	3
III. ELECTRONIC SCANNING OF ANTENNAS USING DIODE-IRISES . . . . .	9
A. INTRODUCTION . . . . .	9
B. THE IRIS CONTROL CONCEPT . . . . .	10
1. Background . . . . .	10
2. Preliminary Investigations With Diode-Iris Controlled Slots . . . . .	12
3. Advantages of Diode-Iris Control . . . . .	18
C. EXPERIMENTAL CONSIDERATIONS AND RESULTS . . . . .	18
1. The Microwave Diode . . . . .	18
2. Diode Selection . . . . .	23
3. Four-Diode-Iris Phase and Amplitude Control Unit . . . . .	25
4. Ten-Element Traveling-Wave Array . . . . .	28
D. REFERENCES . . . . .	42
IV. CONCLUSIONS . . . . .	43
V. RECOMMENDATIONS . . . . .	45



## ILLUSTRATIONS

Figure		Page
1	Iris-controlled slot . . . . .	11
2	Mechanically-controlled complex slot . . . . .	11
3	Experimental phase and amplitude data for mechanical complex slot . . . . .	11
4	Two-diode-iris-controlled slot radiator . . . . .	13
5	Variable amplitude control of test unit No. 3 (diode separation of 0.290 inch) as a function of applied bias voltage of diode No. 3 with bias voltage of diode No. 1 held constant at +0.42 volt . . . . .	15
6	Matching technique for a diode-iris . . . . .	16
7	Diode-iris configurations . . . . .	16
8	Variable phase control of an X-band slot radiator using two varactor diodes . . . . .	17
9	General equivalent circuit representation of semiconductor diode . . . . .	19
10	Simplified equivalent circuit of a continuously operated varactor diode . . . . .	21
11	Equivalent circuits for two extreme bias conditions: (a) forward breakdown voltage; (b) reverse breakdown voltage . . . . .	21
12	Junction capacitance and current as a function of applied bias voltage . . . . .	22
13	Empirical results correlating diode characteristics with microwave device performance . . . . .	24
14	Four-diode-iris phase and amplitude control device . . . . .	26
15	Schematic of phase bridge circuit for testing a single 4-diode-iris control device . . . . .	27
16	Illustration of matching technique employed for a 4-diode-iris control device . . . . .	27
17	Top view of ten-element diode-iris array . . . . .	30
18	Diode and r-f choke holder . . . . .	30
19	Internal views of assembled array with one side-window removed . . . . .	31
20	Diode-iris control panel for ten-element linear array . . . . .	32

21	Phase bridge circuit used for obtaining phase and amplitude distribution in linear array aperture . . . . .	34
22	Rear view of linear array and control panel mounted on turntable . . . . .	37
23	Front view of linear array in ground plane and mounted on turntable . . . . .	37
24	Measured sum patterns illustrating 90 degrees of electronic beam scanning . . . . .	38
25	Comparison of predicted and measured sum and difference patterns for selected scan angles . . . . .	40



## I. INTRODUCTION

This Final Report documents and summarizes the work accomplished in an investigation of advanced antenna techniques for rendezvous and lunar landing radar systems. The purpose of this program has been to study and analyze present and future manned-spacecraft missions requiring rendezvous and lunar landing radar systems. This analysis was made in order to better define the antenna requirements for these missions and to demonstrate the extent to which these requirements can be met within the present state-of-the-art. In conjunction with the latter, recommendations have been made for antenna techniques that show promise in extending antenna technology. One such technique, which employs diode-irises to accomplish electronic-beam scanning, has been investigated and shown to be feasible.

The technical material presented in this report discusses in detail the results of the investigation on electronic scanning using diode-irises. The design and complete electrical performance of an X-band 10-element slot array is given. The linear array, which is designed for a 23 db Taylor distribution, is shown to provide electronic beam scanning over a  $\pm 45$  degree interval about broadside; measured sum and difference patterns are compared with the theory to demonstrate the degree of control that can be obtained. In addition, gain measurements have been recorded to determine the efficiency of the array.

The report includes a summary of the Interim Engineering Report, \* which discussed in detail the requirements to be met by antenna systems that are concerned with earth lunar mission which include lunar rendezvous, lunar landing, and earth rendezvous; and other promising antenna techniques whose development can be expected to provide enhanced performance and flexibility in over-all mission design.

The final section of the Final Report contains recommendations for further investigation and development of a promising antenna technique which can be used to electronically scan an antenna beam.

---

\*"Study of Advanced Antenna Techniques for Rendezvous Radar," Interim Engineering Report P63-75, 31 October 1963.





PRECEDING PAGE BLANK NOT FILMED.

## II. SUMMARY OF ANTENNA SYSTEM CONSIDERATIONS AND REQUIREMENTS

In the discussion of mission profiles, presented in the Interim Engineering Report, an attempt was made to treat those conditions which serve to give bounds to the requirements for r-f sensors. Three segments of manned space missions were discussed primarily from the point of view of the effect these missions have on the requirements of the r-f sensor. The mission segments were lunar orbital rendezvous, lunar landing, and earth orbital rendezvous. An attempt was made to make the description of each mission self-contained. For each mission, a brief description of the mission, the selected representative trajectory, a discussion of the bounds on the parameters, and where appropriate, estimates of acceptable errors on measurements are given. In general, these error estimates were not generated from this study, but were compiled from those sources that were available. The estimates are believed to be representative of the general environment in which the r-f sensor systems that perform missions must operate. Consideration was then given to possible sensor designs, within the state-of-the-art, which could be made to meet the mission requirements. The requirements to be met by antennas are, of course, dependent on the performance necessitated by the mission and on the way the performance is to be achieved by the sensor.

For the rendezvous mission segment, searching and tracking functions must be performed on at least one of the two vehicles involved. The same two functions need to be fulfilled in a lunar landing. Considerations of power, weight, and performance leave little doubt, if any, of the need for a beacon. A beacon will enhance the reliability of the system at a small weight penalty. There are differences in the antenna requirements for beacon antennas placed on a vehicle and on the lunar surface. The most demanding situation, is that for the lunar beacon; this beacon should provide a shaped beam with a maximum near the horizon and a sharp null that, in turn, is situated along the horizon. This requirement necessitates accurate and appropriate siting, as well as suitable design, to avoid multipath problems.

In general, the r-f sensor must search for, acquire, and track a cooperative target in each of the mission segments that were described. The lunar landing mission without a beacon poses a different set of requirements than the beacon-assisted landing or either of the rendezvous missions: the latter represents a point target situation while the former represents the lunar surface. A brief summary of the bounds for pertinent operational parameters is presented in Table I.

Table 1. Summary of bounds on operational parameters for missions.

Mission	Range Maximum (nautical miles)	Range Rate Maximum (feet per second)	Angular Coverage
Lunar rendezvous	445 - 260	4750	110° cone or 110° x 20° fan
Lunar landing beacon assisted	445 - 260	4750	110° cone or 110° x 20° fan
non-beacon	100 (altitude)	1800	—
Earth orbital rendezvous	340	600	50° cone

The requirements on the r-f sensor accuracy were not well established because the functions they were to perform had not yet been completely defined. However, if in the rendezvous missions, the sole purpose of the sensor was to provide range, range rate, and angular rate information to the guidance and control system, then it was established that range and range rate values must be determined to within 5 to 10 percent accuracy, and angular (line-of-sight) rate values must be measured with an accuracy on the order of 0.25 milliradian/second.

If the r-f sensor was used as an altimeter and lateral velocity meter reasonable accuracy requirements would be: altitude 0.5 percent; altitude rate, 1 percent, 0.5 meter/second; and lateral velocity,



2 percent, 0.5 meter/second. Here primary consideration has been given to the establishment of accuracy requirements for a landing velocity less than 1 meter/second and minimization of the fuel expended for main braking thrust.

It was observed that in many respects conventional airborne radar and radio navigation techniques are highly suitable as rendezvous and lunar landing radar systems. A minimum of modification is needed to provide equipment, including the antenna, that is at least workable. This conclusion stems from two pertinent considerations. First, many of the requirements to be met by the r-f sensor in the rendezvous and landing maneuvers are very similar both in function and accuracy to those imposed by the airborne situation. Second, and very important from a practical standpoint, airborne navigation and radar equipment has been subjected to extensive and intensive research development, and manufacturing efforts with the aim of improving performance and reliability and of reducing weight, volume, and power consumption.

The essential requirements imposed on sensors by the mission segments, particularly when considered alone can be met with relatively conventional state-of-the-art components and radio frequency equipment. However, when the overall requirements of the mission including such factors as weight, no moving parts, high directional capability, large scan angles are taken together, it is apparent that other techniques should be considered. Electronic scanning has the possibility of eliminating some of the short-comings of the mechanical scanned antenna system. For these reasons electronic scanning techniques and stowable antenna methods were studied in detail in this program.

In the Interim Engineering Report two specific electronic beam steering techniques and several stowable antenna methods were discussed.

One of the most promising techniques for implementation of complete electronic control (in both phase and amplitude) over the radiation from a slot array is the use of a diode-iris configuration in a slotted waveguide. A semiconductor material is used as the key control device at each element of the array. A direct current bias is applied to each

of four diodes to control the symmetry of the electric field exciting a slot in the broadwall of a waveguide. The details and background of this type of electronic control, in addition to some of the experimental results with a 10-element linear array are thoroughly described in the subsequent section of this report.

It was shown that antenna beam pointing can also be accomplished through control of only the amplitude of excitation of the individual elements of an array. A specialization of this technique requires that the received energy in the antenna elements be modulated ON and OFF at a suitable repetition frequency and that a controllable 180 degree phase reversal be associated with each element. Thus, the scanning can be accomplished by synthesis of the pattern in a different region of space as a function of time by a binary coding of ON-OFF switches.

A laboratory model of an amplitude scanning array was shown to have been constructed and operated at the Hughes Aircraft Company. This early version, which is a linear array operating in receive only, has the growth potential for two-dimensional scanning and two-way operation. Although the technique can be used in both transmit and receive, its application to the cooperative rendezvous mission would require that the system track a beacon and consequently the present capability for reception only, might be adequate for this purpose.

The general theory of the time-modulation amplitude scanning technique and the application in a possible system was discussed. In addition, the experimental verification at X-band was described. A system description that includes the radiating aperture, the switches, and the electronic controls and read-out circuits in a lightweight and compact form may become a worthwhile effort in the future of this present program. This technique has possible applications to a number of situations that call for complete electronic scanning without the use of phased arrays.

The variety of situations implicit in the lunar mission profiles that were studied called for the consideration of antenna configurations different from the conventional, rigid, stowable types that have been required for space missions. Antennas can be designed which, when

packaged, occupy small volumes during launch-boost and which subsequently can be unfurled by mechanical means or gas pressure. Although these antennas have the obvious advantages of large size-to-weight ratio, the questions of reliability and performance remain largely unanswered at present because the necessary analysis, construction, and testing has not been carried out. Preliminary investigation of unfurlable antennas should involve analytical and experimental studies for the determination of the random and systematic errors typical of each particular design. In addition, demonstration models of equipment for optical alignment of antennas should be built and tested. The reliability and relative performance may then be inferred from these data.

It has been shown that, for a tracking and acquisition radar for lunar rendezvous operating in the normal beacon-assist mode, a relatively small, conventional rigid antenna is sufficient. However, it may be essential that the radar have the capability of functioning normally without a beacon. One of the methods by which this mode of operation may be achieved is by an increase in the antenna gain. This method implies a larger physical aperture if all other parameters remain the same.

For the skin-track (no beacon) case, then, it is useful to consider unfurlable antennas that are characterized by elements of a filmy or spidery nature. Unfurlable antennas are conveniently classified according to the means employed for extension to the operational configuration. The term "erectable" is used here to describe antennas that are erected by mechanical means; the term "inflatable" is used to describe antennas which are made to take their shapes by means of gas pressure.

For applications which require that the antenna be furled and unfurled repeatedly, it is necessary that the antenna be mechanically erectable since no provision can be reasonably made for deflation and folding of a pliant, filmy structure in space. Both reflector and array antennas can be adapted to this requirement, so that it is useful to discuss the characteristics of each from the point of view of their



respective adaptabilities. Here, fairly rigid members are arranged to form the radiating surface and the feeding structure. Three types of erectable antennas were suggested and were discussed:

1. Planar arrays of slots.
2. Arrays of small end-fire elements, each of which has gain itself.
3. Erectable paraboloids.

Inflatable arrays and reflectors are balloons of metalized film cut and shaped according to the proper pattern. Inflation is accomplished with a bottled gas source or, alternatively, with a solid material that sublimates under excitation by ultra-violet radiation. Means may be provided for rigidization of the antenna surface subsequent to inflation: there are materials systems which can be applied to the film prior to packaging and which, on deployment of the antenna, react to form a lightweight rigid backing for the antenna surface. Some stiffening may also be accomplished simply by taking advantage of the work-hardening effect of inflation upon the aluminum foil which is part of the film.

Of the two types of highly directive antennas, reflector antennas and arrays, the former was shown to be nearer realization as an inflatable antenna for space vehicle application. There are several reasons:

1. The paraboloidal or circular reflector shapes are perhaps more natural for inflation than are the characteristically flat or slightly curved surfaces of arrays.
2. The feed arrangement for a reflector is simpler, particularly for paraboloids.
3. Work on inflatable reflectors has been spurred by the need for large, lightweight solar concentrators.

Several types of inflatable reflector antennas and their design and construction techniques were discussed along with some preliminary results concerning expected accuracies of construction and electrical performance.

### III. ELECTRONIC SCANNING OF ANTENNAS USING DIODE-IRISES

The following section of this report describes in detail the diode-iris control concept and the results obtained to date with a 10-element slot array operating at X-band. The linear array is shown to provide electronic beam scanning over a  $\pm 45$  degree interval about broadside.

#### A. INTRODUCTION

Electronic beam steering of an antenna aperture composed of discrete radiating elements is accomplished by suitably adjusting the phase of excitation at each element. In a linear array of equi-spaced elements the phase must be shifted by the same amount at each radiator to collimate the beam in a given direction in space. This phase shift is accompanied by changes in the pattern beamwidth and gain with changing beam position. Electronic scanning has found application historically in interferometer techniques for radio astronomy and, more recently, in ground and ship based radars. This latter application is the aim of much current development work at the Hughes Aircraft Company. However, the implementation of techniques for electronic control, that are appropriate for space radars, is still beyond the present state-of-the-art although several techniques show promise for future application in lightweight electronic scanning antennas.

A straightforward method of electronic scanning consists of the insertion of phase shifters at, or in series with, each radiating element. Phase control may be accomplished with a variety of devices, ranging from mechanically actuated loads which long have been employed for this purpose, to the more recent designs using ferrites or semiconductor materials. At lower frequencies, ferrite phase shifters have been used as a standard component of large ground or ship-based radar arrays for the past several years. More recently, low loss ferrites which can be used as phase shifters in the upper end of the microwave band have been developed. These devices require large magnets and are very temperature sensitive. One of the most promising of phase shifting devices is

a slot radiator device which employs varactor diodes in an iris control configuration. The implementation of a diode as a waveguide iris for control of phase and/or amplitude for an electronic scanning antenna is discussed in this section.

The advantages of electronic steering over mechanical steering lie in the elimination of movement and the mechanical problems associated with moving parts. Rapid movement of the beam is inherent in most electronic scanning techniques. As one consequence, high-speed data processing has become possible although the system implication of such a capacity has not yet evolved.

## B. THE IRIS CONTROL CONCEPT

### 1. Background

The idea of using a waveguide iris configuration for control of the radiation from a slot is relatively new. Control of this type was first demonstrated by Tang<sup>1</sup> who used a single, mechanically-operated metal iris to control the amplitude of slot radiation over a 50 db range at X-band. The device is illustrated in Figure 1. It consists of a longitudinal, centered broadwall slot and a resonant metallic iris which is inserted into the guide through non-radiating slots in the narrow walls and driven by a micrometer mechanism. When the iris is positioned symmetrically in the waveguide, the slot does not radiate; as the iris is moved to one side or the other, the slot radiates with an amplitude dependent on the iris displacement. Iris-controlled elements of this type have been successfully used in linear arrays to produce a variety of radiation patterns.

The most general type of broadwall slot is that which is displaced and inclined from the centerline of a waveguide. Maxum<sup>2</sup> has shown that this "complex" slot couples to both series and shunt currents in the waveguide broadwall and thus is capable of providing phase and amplitude control. It was demonstrated that two resonant metallic-irises (Figure 2) could successfully be used for mechanical control of a complex slot. Figure 3 illustrates the experimental amplitude (40 db range) and phase (180 degree range) control that was obtained by operation of the device

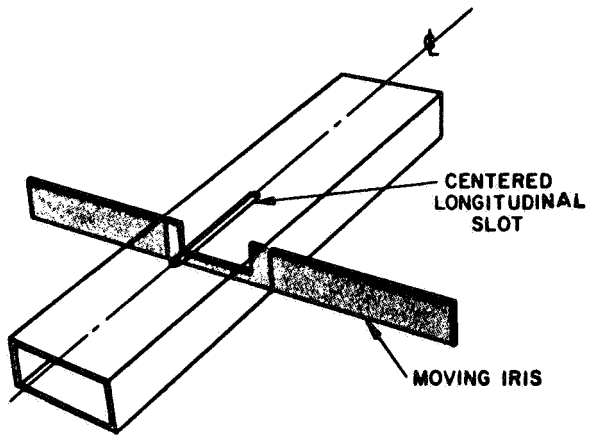


Figure 1. Iris-controlled slot.

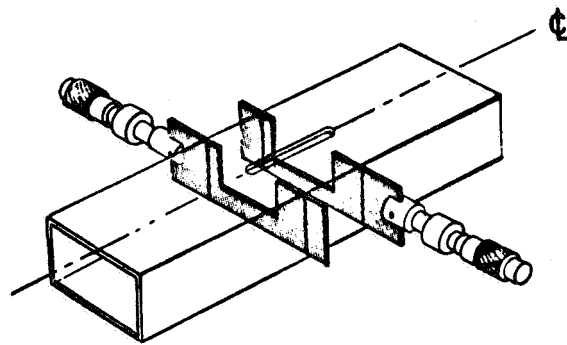


Figure 2. Mechanically-controlled complex slot.

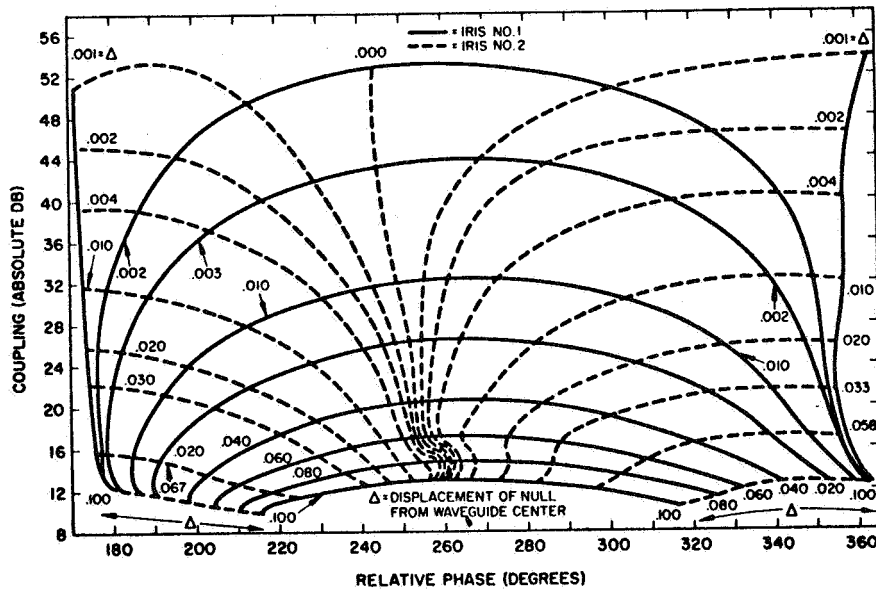


Figure 3. Experimental phase and amplitude data for mechanical complex slot.



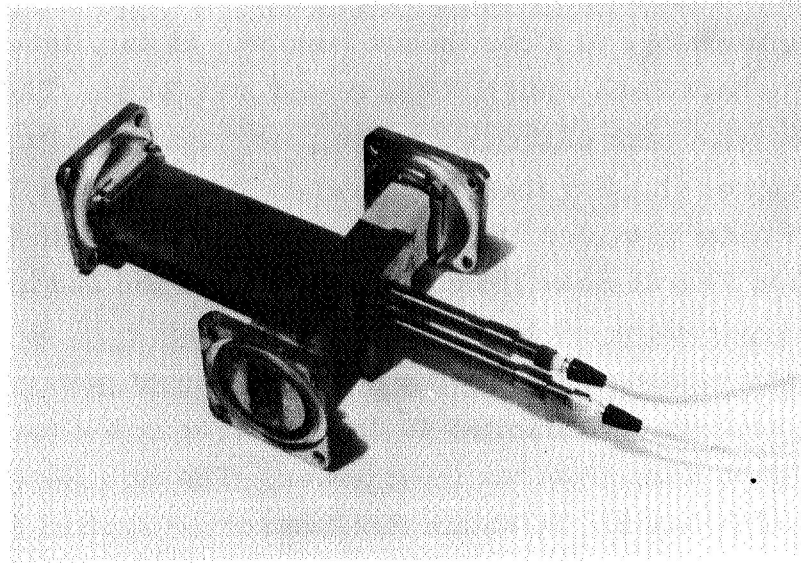
over only a portion of its range; the solid and dashed lines indicate constant settings for irises No. 1 and No. 2, respectively. Operation of the device over the complete iris displacement range can give 360 degrees of phase control.

These techniques can be adapted to electronic control by the use of either ferrite<sup>3</sup> or semiconductor irises. For the ferrite device the control mechanism is a d-c magnetic field provided by an externally mounted electromagnet. Two types of ferrite-excited slots at X-band have been developed: one in which the amplitude of the radiation is controlled over a 40 db range (maximum normalized coupling: 0.25) and another in which both amplitude (0 to 40 db) and phase (0 to 360 degrees) can be controlled. However, several major problems are encountered in adaptation of this technique to control the excitation of a multi-element slot array: The physical size of the electromagnets necessary to obtain the above control is incompatible with the interelement spacing of the slots. Interaction between magnetic control circuits of adjacent slots has to be resolved. Relatively high currents (on the order of amperes) are required for adequate control, and the electromagnets are bulky and quite heavy.

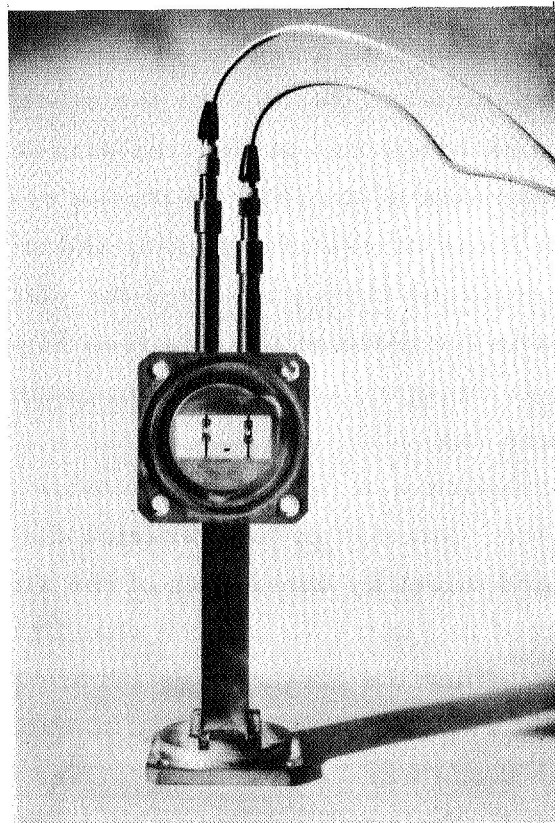
## 2. Preliminary Investigations With Diode-Iris Controlled Slot

To overcome the shortcomings of the ferrite devices, an investigation has been conducted at the Hughes Aircraft Company which employs commercially available diodes as the iris control element. Here the control mechanism is a voltage which is supplied by a 6 volt dry cell battery. The initial investigation with the diode iris dealt with control of the amplitude and phase of radiation from a slot at X-band. The iris consisted of two symmetrically disposed varactor diodes which lay in a transverse plane of the waveguide. On the broadwall opposite the slot arm, two r-f chokes were mounted to permit the diodes to be externally biased as shown in Figure 4. The devices to be discussed in the next paragraph were designed for amplitude control alone.

The operation of the device was based on the principle that a variation of the electrical characteristics of one diode with respect to the



(a)



(b)

Figure 4. Two-diode-iris-controlled slot radiator.

other distorts the current density in the vicinity of the slot and causes its coupling to change in a continuous fashion. So far, three amplitude control units have been designed and tested at X-band. They are three-port devices with each of the two output ports terminated in a matched load (see Figure 4). For this configuration the 1st unit (0.548 inch diode separation) provided 28 db of amplitude control with the maximum slot radiation 19.6 db down from the input power; the 2nd unit (0.450 inch diode separation) exhibited 36 db of amplitude control with the maximum slot radiation 14.3 db down from the input power; the 3rd unit (0.290 inch separation) exhibited 44 db of control with a maximum slot radiation 6.2 db down from the input power. The data for this last unit are shown in Figure 5. To obtain this control the applied d-c bias across a diode is carried through about a 6 volt range. The diode driving power is on the order of microwatts. The phase deviation is less than 10 degrees for the complete amplitude swing, a result which indicates the existence of a high degree of physical symmetry in the structure. The experimental results for the other two units are similar.

Additional work which was performed with the 3rd unit included impedance measurements of the iris. With the results of these measurements, a method was devised for making the iris resonant; the scheme that was employed simply involved the placement of a tapered capacitive element in the plane of the iris (see Figure 6). The device discussed above was designed to achieve amplitude control from a slot radiator (see Figure 7a).

Another test device was designed to provide phase control primarily. This device consisted of two varactor diodes placed in a transverse plane and offset by one-fourth of the slot length. The configuration is depicted in Figure 7b and the phase change obtained is shown in Figure 8. When the bias voltage across a diode was changed, the phase of the slot radiation was observed to vary  $\pm 87$  degrees, depending on which diode was being biased. Over this phase control range, the variance of the amplitude was about 13 db, which indicates

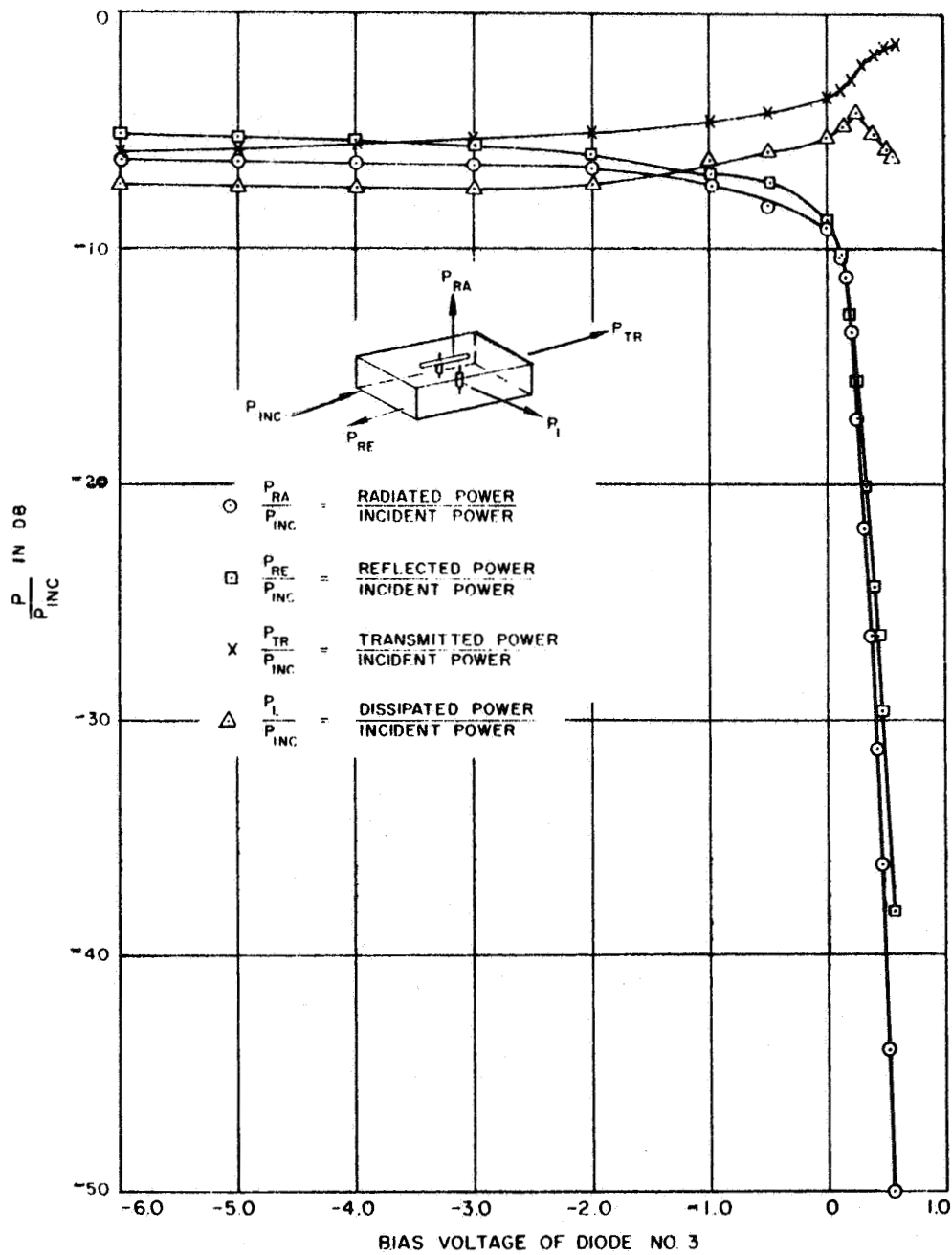


Figure 5. Variable amplitude control of test unit No. 3 (diode separation of 0.290 inch) as a function of applied bias voltage of diode No. 3 with bias voltage of diode No. 1 held constant at +0.42 volt.

$f = 9.375 \text{ Kmc}$

Unit matched for zero reflection at nonradiation condition (-50 db)



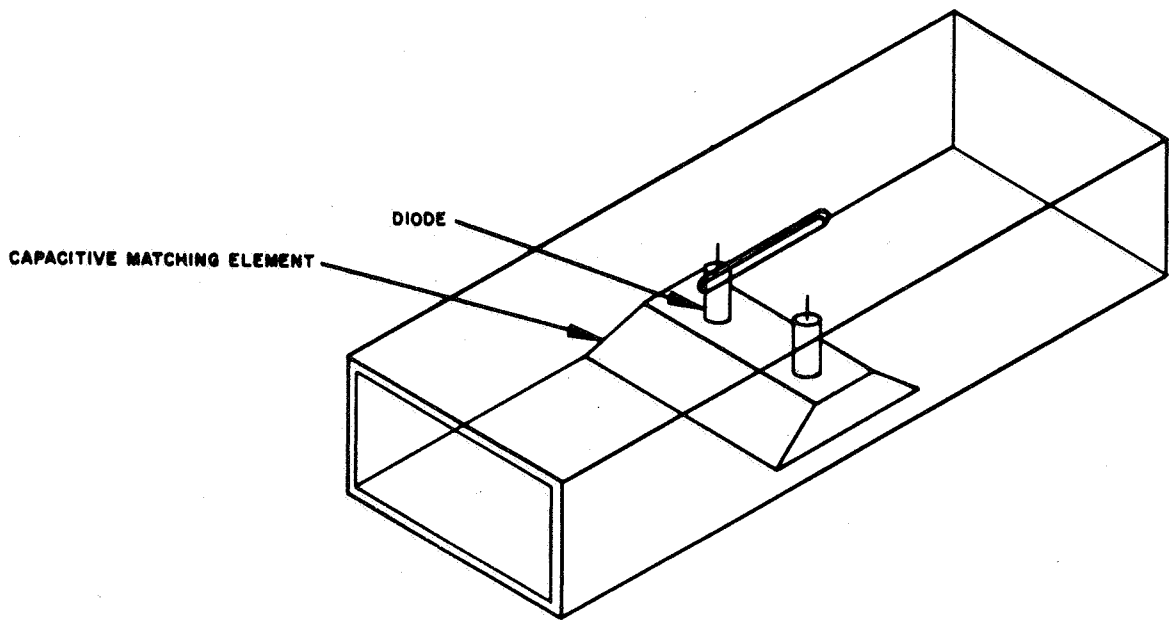
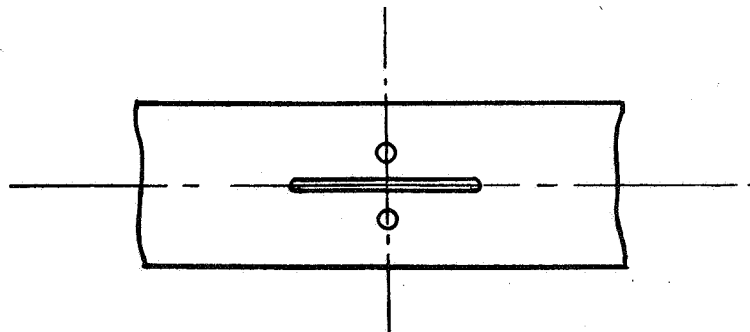
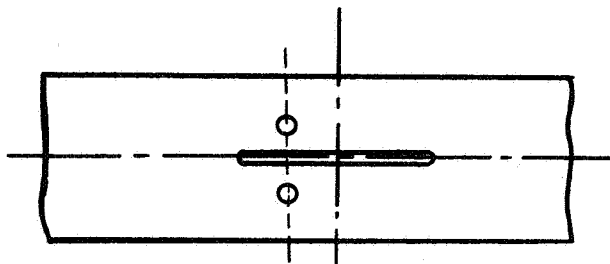


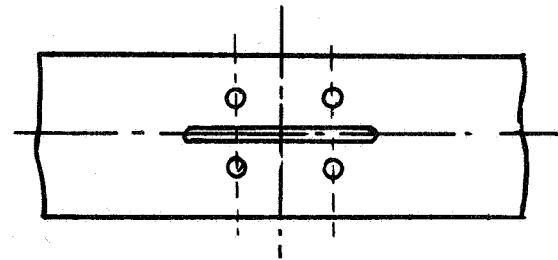
Figure 6. Matching technique for a diode-iris.



a) for variable amplitude control



b) for variable phase control



c) for variable phase and amplitude control

Figure 7. Diode-iris configurations.

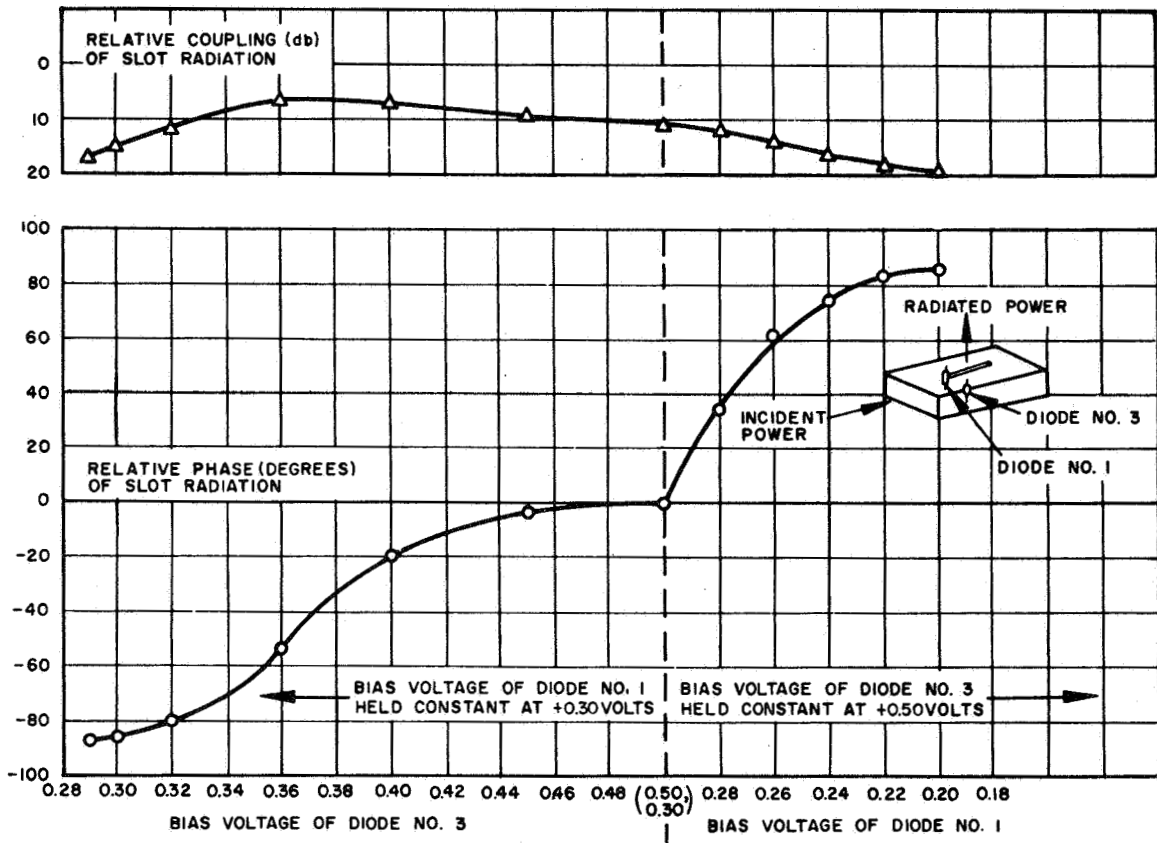


Figure 8. Variable phase control of an X-band slot radiator using two varactor diodes.  $f = 9.375 \text{ Kmc.}$

that insufficient control is being exerted on the amplitude in this configuration.

### 3. Advantages of Diode-Iris Control

The development of a diode-iris configuration to control the phase and amplitude of a slot radiator will provide electronic beam scanning and arbitrary pattern synthesis or beam shaping for a multi-element slot array with the following advantages:

1. A physically compact control circuit which is compatible with the interelement spacing of the slots.
2. A lightweight control circuit.
3. Electrically isolated control circuits between adjacent elements.
4. Control circuits which require relatively low driving powers.
5. A capability to rapidly change the radiation characteristics of an antenna.

## C. EXPERIMENTAL CONSIDERATIONS AND RESULTS

### 1. The Microwave Diode

Semiconductor devices can be described theoretically in terms of their physical properties and nonlinear electrical behavior. In microwave applications it is found more convenient to describe the characteristics of such devices by their equivalent linear-lumped parameters. Representations using simple looking equivalent circuits have therefore been devised in an attempt to represent this nonlinear device at microwave frequencies. Although these representations are good only over a very limited range of frequencies and limited range of bias conditions, the values of the measured lumped parameters for the device allow accurate prediction of its performance in many applications. A general representation for a variable reactance semiconductor diode, in this

case a varactor,\* is shown in Figure 9. The diode parameters,  $L$ ,  $C_j$ ,  $C'$ ,  $R_s$ , and  $R_b$ , and  $\omega$ , are defined as follows:

- $L$  = whisker and lead inductance
- $C_j$  = junction (or barrier) capacitance
- $C'$  = parasitic and holder capacitances
- $R_s$  = spreading resistance
- $R_b$  = nonlinear barrier resistance
- $\omega$  =  $2\pi f$  where  $f$  = frequency

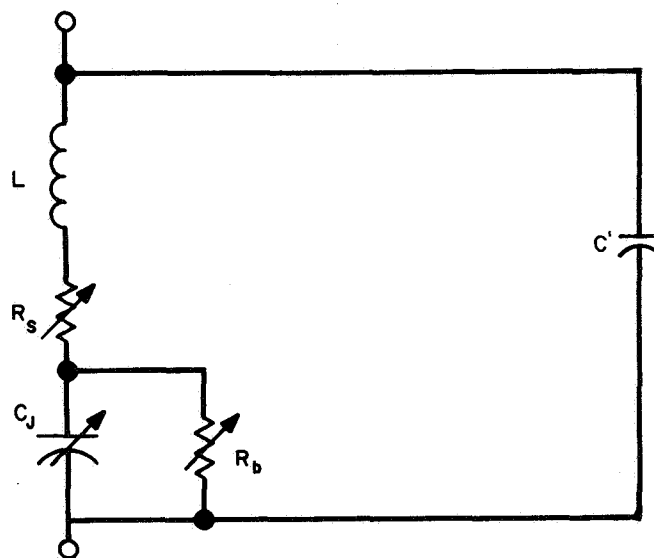


Figure 9. General equivalent circuit representation of semiconductor diode (arrows indicate dependency on bias).

\*The varactor diode is a p-n junction diode characterized by its large range of capacity variation with applied bias voltage. The name "varactor" has been proposed for any device whose major characteristic can be represented by a nonlinear reactance.



Since the shunt capacitance  $C'$  and series inductance  $L$  can be assumed to be tuned out by the diode holding mechanism, the circuit of the microwave diode can be simplified further; also, the value of  $R_b$  is much larger than the junction reactance  $X_c = (1/\omega C_j)$  at the high frequencies used here so that it too can be ignored. The variation in capacitance with the applied bias voltage  $V$  across the diode is given by the approximate relation<sup>4</sup>

$$\left(\frac{1}{C_j}\right)^n = K(\phi - V) \quad (1)$$

where  $K$  and  $\phi$  are constants, and  $n$  is around 2 for a step-junction and around 3 for a diffused junction. From this relation it is seen that the reactance associated with  $C_j$  approaches zero as the forward bias voltage  $V$  approaches  $\phi$ . In summary, a diode which is operated over its bias range can be represented by the equivalent circuit of Figure 10; the representations for the extreme forward and reverse bias conditions (i. e., for forward and reverse breakdown voltages) and the corresponding current flow can be drawn as in Figure 11a and 11b. To indicate how a typical diode behaves electrically, the junction capacitance  $C_j$ , and the junction current  $I$ , are plotted as a function of voltage in Figure 12.

A quality rating, or figure of merit for a varactor diode, stated by Houlding, is given by the formula

$$f_c = \frac{1}{2\pi R C_{j\min}} \quad (2)$$

where  $f_c$  is called the cutoff frequency;  $R$ , the equivalent series resistance, and  $C_{j\min}$ , the minimum junction capacitance, are measured at reverse breakdown. An equivalent figure of merit is the  $Q$  of the diode which can be expressed as

$$Q = \frac{f_c}{f} \quad (3)$$

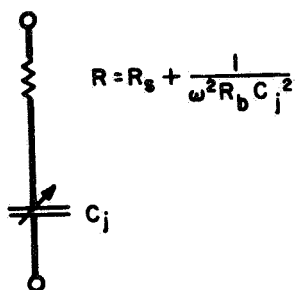


Figure 10. Simplified equivalent circuit of a continuously operated varactor diode.

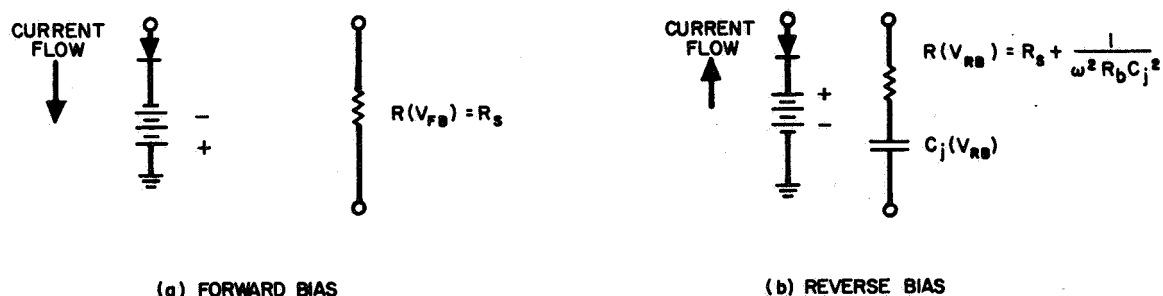
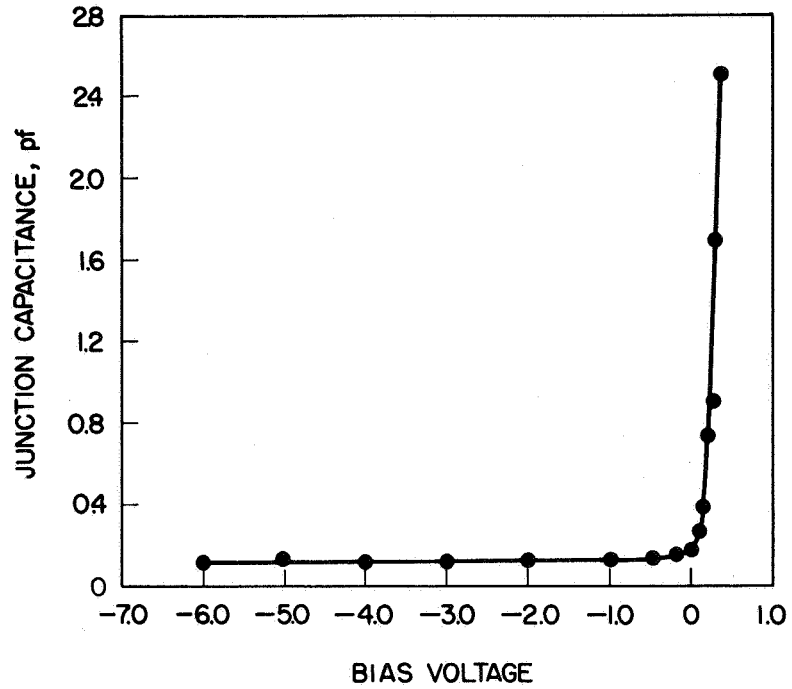


Figure 11. Equivalent circuits for two extreme bias conditions: (a) forward breakdown voltage; (b) reverse breakdown voltage.

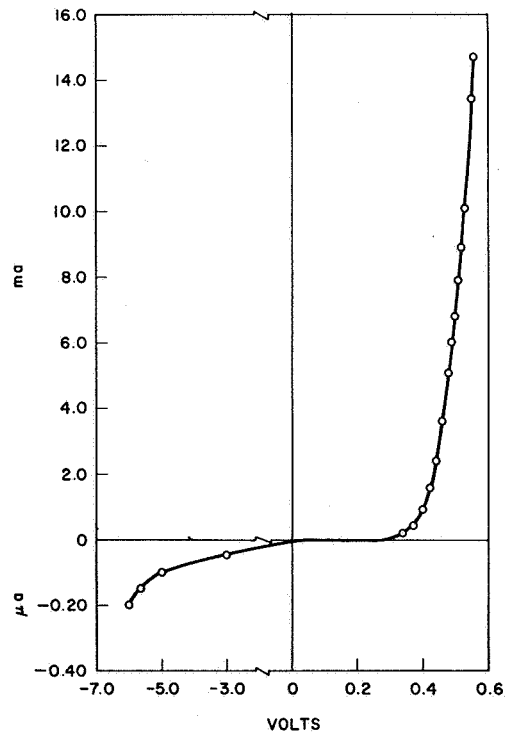
where  $f$  is the frequency at which  $R$  and  $C_{j\min}$  are measured. These parameters just defined give a convenient, useful, and accurate description of the diode. The details of the method of measuring these parameters are not sufficiently standardized to make possible direct comparisons between the products of various manufacturers.

A high  $Q$  can be achieved if a minimum  $RC_{j\min}$  product is realized. To get the maximum capacitance change,  $C_{j\min}$  should also be minimized. Due to the physical geometry, a compromise must be made between the values of  $R$  and  $C_{j\min}$ . The junction capacitance is directly proportional to the area of the junction, while  $R$  varies approximately inversely with the junction area for a mesa (distributed) junction diode and inversely as the circumference of the area for a point contact diode.

Semiconductor diodes are especially attractive for high frequency use because of their small dimensions, fast response, and low noise. Since the diodes are physically small, they can serve as variable



(a) Diode junction capacitance versus voltage.



(b) Diode current versus voltage.

Figure 12. Junction capacitance and current as a function of applied bias voltage.

reactance elements in shunt or in series in a waveguide transmission line and still be matched to the waveguide. The essential purpose of using varactor diodes, then, in microwave phase shifters, is to exploit the extremely large range of reactance available.

## 2. Diode Selection

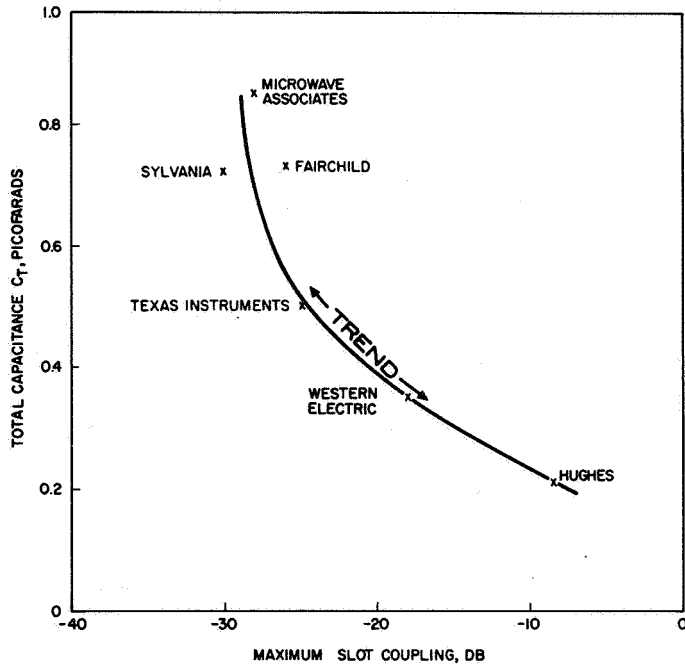
In order to select the diode most suited for this device it was found necessary to conduct a comparative study of commercially available varactor diodes. The objective of the study was to establish a correlation between the diode characteristics and their influence in optimizing the microwave device performance. Diodes of different manufacture and possessing various package and junction designs were investigated; all were of the varactor family and included samples from Fairchild, Hughes, Microwave Associates, Sylvania, and Texas Instruments. To establish the desired correlation, an empirical technique was employed. This technique consisted of (1) using Houlding's method<sup>4</sup> to measure diode characteristics such as cut-off frequency, minimum total capacitance\* and series resistance, and (2) inserting a pair of closely matched diodes into the variable amplitude control unit (2-diode-iris unit) and measuring the degree of slot coupling and the dissipative insertion loss introduced by the diodes.

The results obtained for the various diodes used in this study are given in Figure 13.

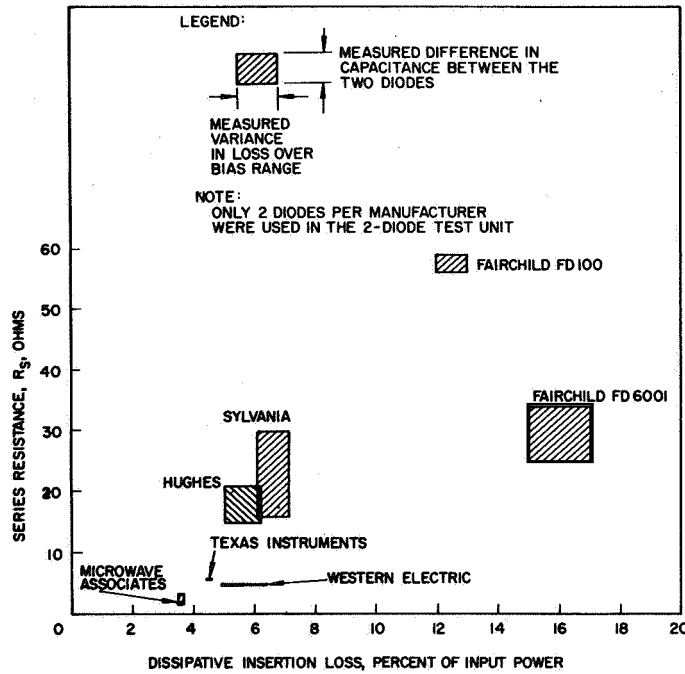
The VSWR varied from 5:1 for the Hughes diodes to values greater than 10:1 for all other brand diodes, with the exception of Fairchild's glass package computer diode which displayed a VSWR of 8:1. Despite this level of mismatch, definite trends appeared in the slopes of the two curves presented. These trends indicate that (1) lower minimum diode capacitance values, as seen in the waveguide, will result in greater ranges of coupling control, and (2) lower diode series resistance values will substantially decrease the dissipative insertion loss of the device.

---

$$*C_{\text{total}} = C_{\text{junction}} + C_{\text{package}}$$



(a) Total diode capacitance,  $C_T$ , at -6 volts versus maximum slot coupling.



(b) Series resistance of diode,  $R_S$ , at -6 volts versus dissipative insertion loss.

Figure 13. Empirical results correlating diode characteristics with microwave device performance.



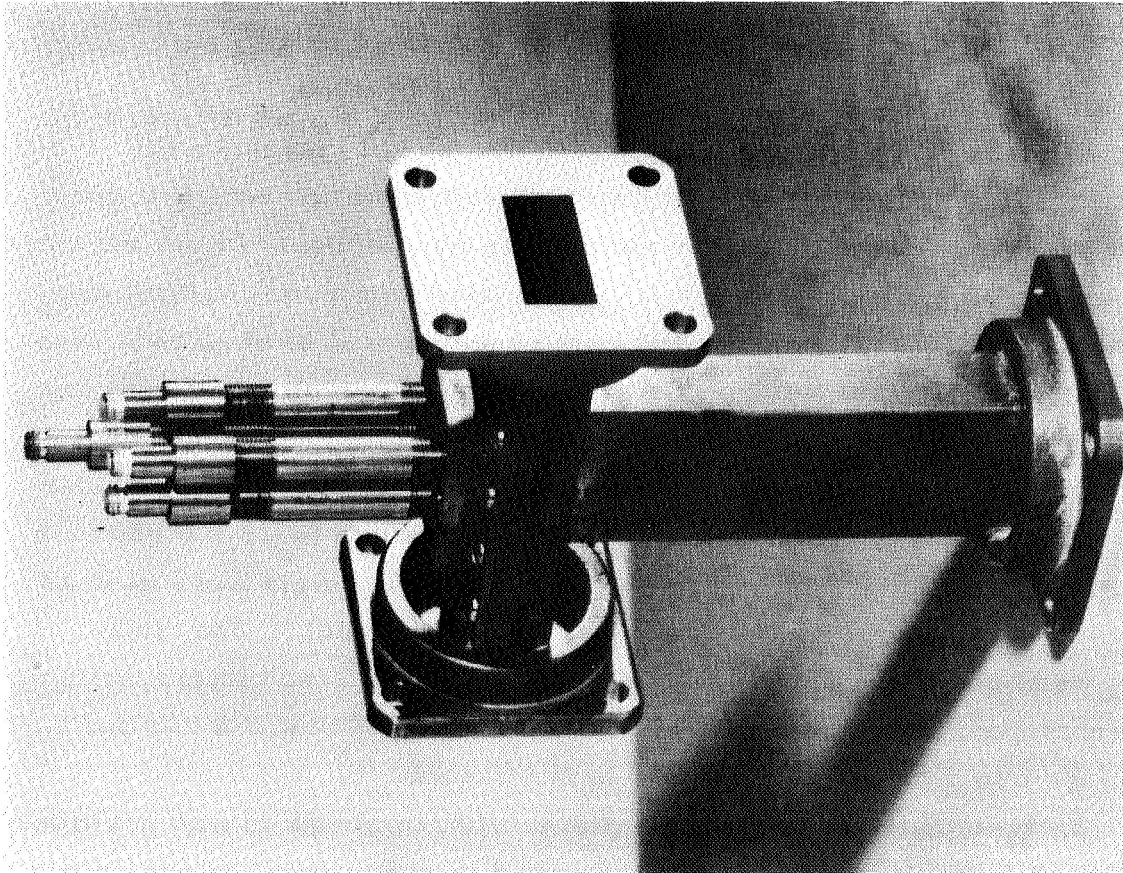
Thus, varactor diodes with high Q ratings<sup>5</sup> ( $Q = 1/2\pi fR_S C_j$ ) are required in the diode-iris slot radiator application. The Hughes silver-bonded germanium type diodes have the highest Q values ( $Q > 20$  for -6 volts at 10 Kmc) among all diodes tested; this rating in conjunction with their ability to provide the maximum range of coupling control made them best fitted for further study in the diode-iris investigation.

### 3. Four Diode-Iris Phase and Amplitude Control Unit

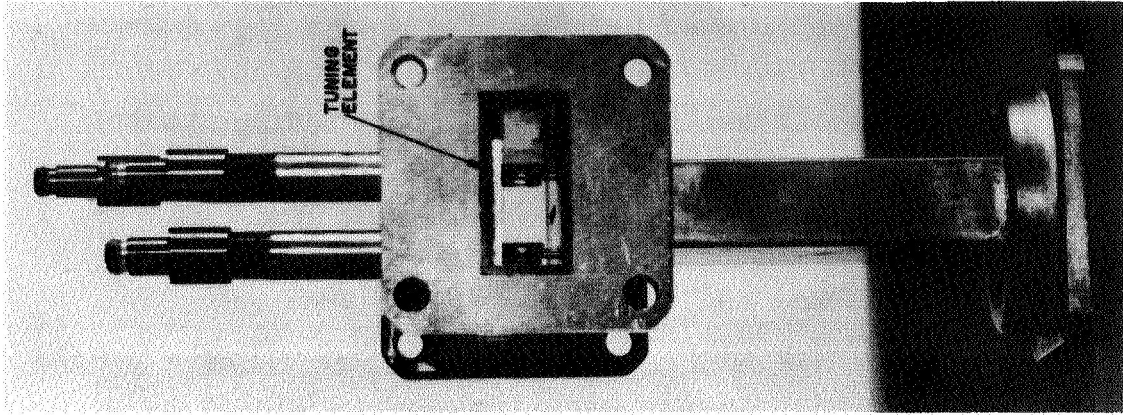
Previous diode-iris devices described in this report have utilized two diodes to demonstrate either amplitude control or partial phase control over the radiated field from a slot in a waveguide. The device to be described in this section employs a four-diode configuration which demonstrates complete phase control in addition to independent amplitude control. Experimentation was conducted at 9.375 Kmc with Hughes diodes of the Silver-bonded Germanium type (HD-5610). Photographs exhibiting the diodes and their chokes in the assembled test unit are shown in Figure 14.

A phase bridge shown in Figure 15 was used to measure the relative phase and amplitude variations of slot radiation as a function of the dc voltage settings across each of the four diodes. Initial readings with an unmatched unit (VSWR  $\approx$  10:1) indicated continuous control of phase over a 360-degree range and continuous control of amplitude over a 30 db coupling range with maximum coupling at -22 db relative to the input power. Efforts were directed toward matching the unit to the characteristic impedance of a standard rectangular waveguide. Rectangular brass slabs one-half guide wavelength in length ( $\lambda_g/2 = 0.880$  inch at 9.375 Kmc), 0.900 inch in width, and of variable height were used as capacitive step tuners to obtain the best possible match. The diode pairs were positioned on the slab with a  $\lambda_g/4 = 0.440$  inch interspacing; this interspacing was chosen so that the reflections from the two pairs of diodes would be out of phase and hence cancel.

Each diode in the transverse planes of the waveguide was positioned 0.225 inch from the narrow wall, i. e. , at a distance equal to one-fourth of the guide width (see Figure 16).



(a)



(b)

Figure 14. Four-diode-iris phase and amplitude control device.

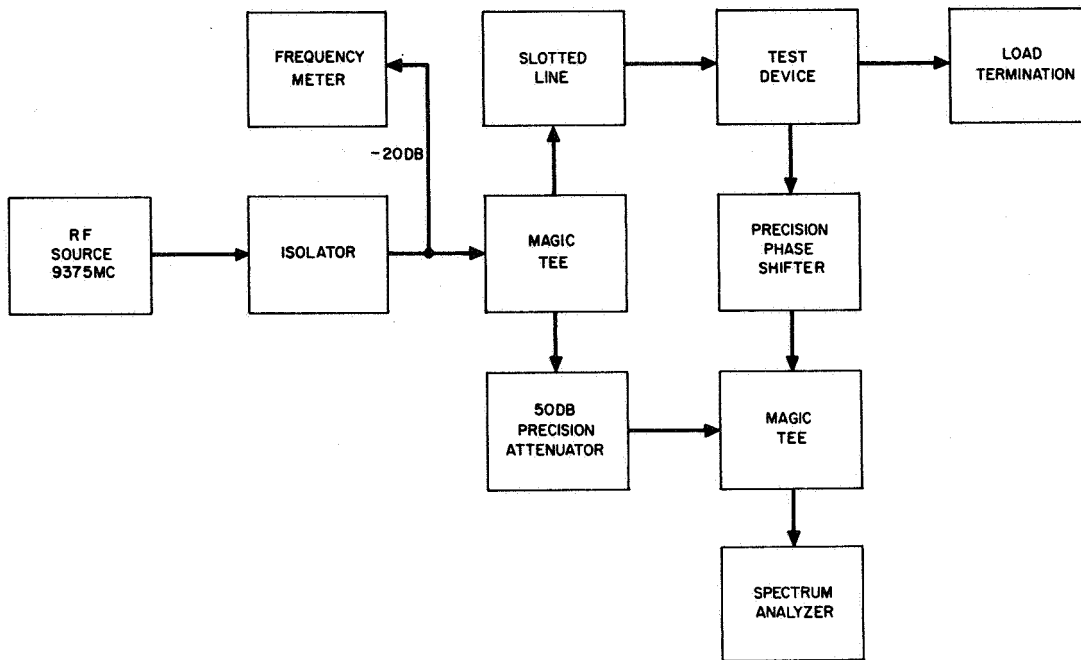


Figure 15. Schematic of phase bridge circuit for testing a single 4-diode-iris control device.

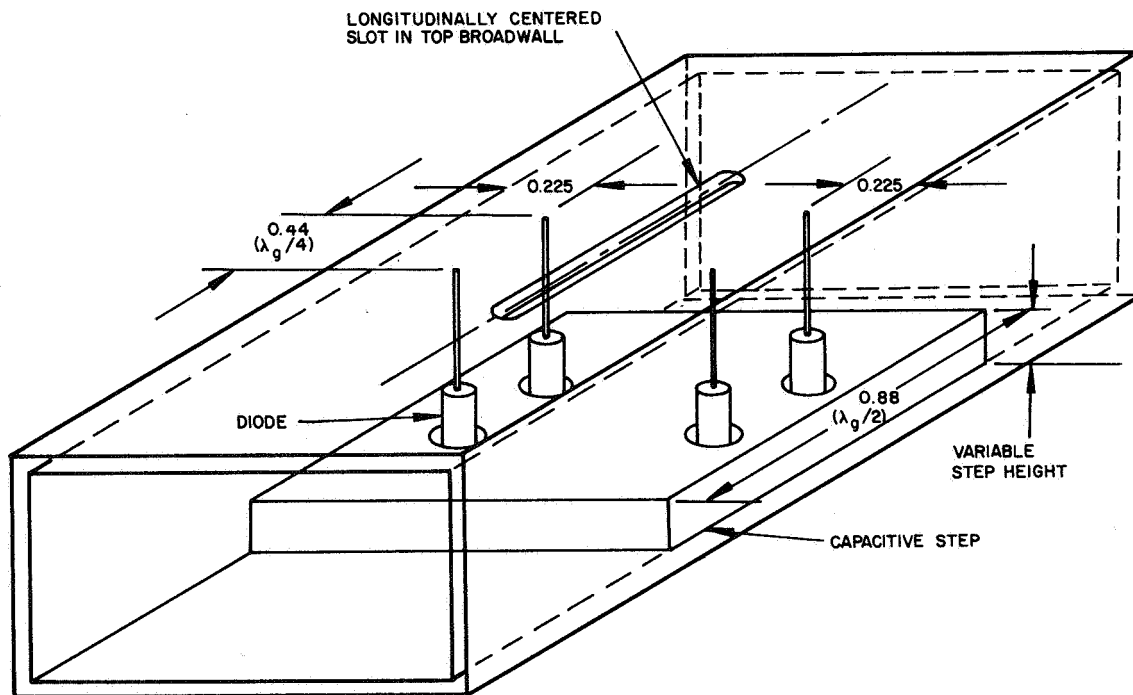


Figure 16. Illustration of matching technique employed for a 4-diode-iris control device.

A slab depth which corresponded to minimum VSWR for the condition of minimum slot coupling was determined; this depth was found to be about 0.140 inch which corresponds to a reduction in waveguide height from 0.400 to 0.260 inch. The VSWR for -50 db coupling (minimum coupling) was 1.19:1 and less than 1.4:1 over nearly the entire control range for the four-diode device. Amplitude coupling control to -15 db was observed with a phase control range of 360 degrees. At minimum slot coupling the insertion loss was 1.4 db; the extreme values of insertion loss were measured to be 1.1 db and 1.8 db at -36 db coupling (VSWR = 1.39:1) and -9.1 db maximum coupling (VSWR = 1.10:1), respectively. These results show that a significant improvement in device performance was obtained through impedance matching.

An additional measurement was made to determine the variation in phase of the wave transmitted past the device. A phase variation of less than 30 degrees was observed which was taken into account in establishing the phase of the slot excitations in the ten-element array.

It should be emphasized that full control of the slot radiation characteristics is accomplished with merely microwatts of driving power. Furthermore, these ranges of control were accomplished without exceeding the forward or reverse breakdown voltages of the diodes. The breakdown voltages for these diodes are:

$$\text{Forward Breakdown} = V_{FB} = +0.52 \text{ volts at } 10 \text{ ma.}$$

$$\text{Reverse Breakdown} = V_{RB} = -6 \text{ volts at } -100 \mu\text{a.}$$

The diodes were observed to draw a negligible amount of current when operated between  $V_{RB}$  and  $V_{FB}$ .

#### 4. Ten-Element Traveling Wave Array

Antenna Components. From the results with a single four-diode-iris control unit, the design, fabrication and testing of a 10-element traveling-wave array was undertaken. The linear array proper consisted of a milled-rectangular waveguide fixture of width 0.900 inch and height 0.260 inch, whose top plate contained 10 uniformly spaced slots on the center line, and forty Hughes diodes with provisions made in the waveguide

fixture for the insertion and securing of the diodes to the waveguide (see Figure 17). Removable windows in the waveguide narrow wall were used to facilitate precise adjustment of the position of the diodes and to ensure reliable electrical contact for both lead wires of the diode. Pressure fitting of the lead wires into holes drilled to the wire diameter was employed where necessary to secure good contact. Figure 18 shows one lead wire (anode terminal) of a typical diode being connected to the center conductor of its r-f choke assembly by means of an 0-80 set screw; in Figure 19 the other diode lead wire is shown to be pressure-fitted through a hole in the waveguide broadwall which contains the slots; silver paint was used in the holes to ensure good electrical contact. The slot interspacing  $\underline{d}$  was chosen to be  $0.586 \lambda_0$  or 0.738 inch in order to accommodate a reasonable spacing between consecutive four-diode-iris clusters. The reduced height waveguide array utilized linear-tapered transitions as impedance transformers at its ends to provide a smooth transition into standard X-band waveguide test equipment. The VSWR for each transition was about 1.05:1.

In addition to the array proper, diode-bias control circuits were designed and fabricated. These circuits contained 40 precision, 10-turn potentiometers which permitted independent, manual control of the dc voltage across each of the 40 diodes in the array. The potentiometers were mounted in a common control panel as shown in Figure 20; polarity switches were located directly above each potentiometer to provide forward and reverse biasing of the diodes. The control panel also included an ammeter to monitor individual diode current in the forward bias direction; and a voltmeter to monitor the voltage across the diodes. Necessary switching circuits were also provided. Two regulated dc-power supplies were used.

Aperture Distributions. The demonstration of electronic scanning included the generation of sum and difference patterns at selected positions in space in a 90-degree angular sector. Seven aperture distributions, in all, were set up with the diode-irises. The aperture phasing was selected to generate sum patterns at  $\theta = 0$  degree,

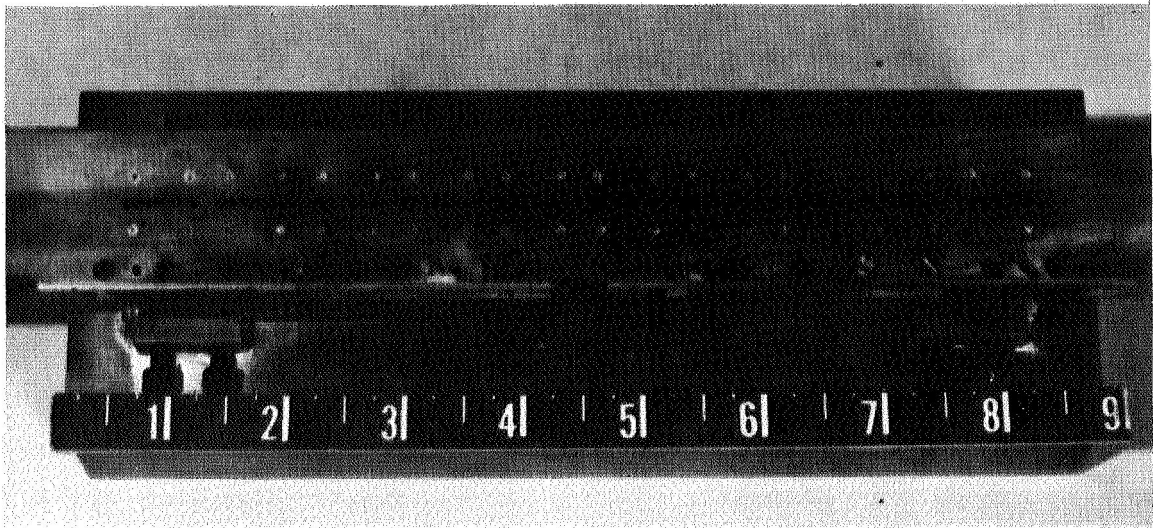


Figure 17. Top view of ten-element diode-iris array.

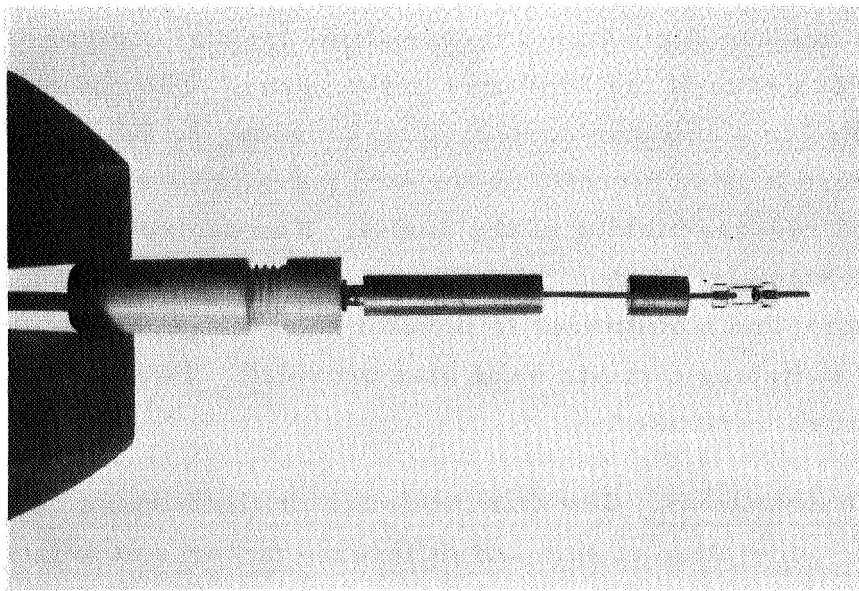
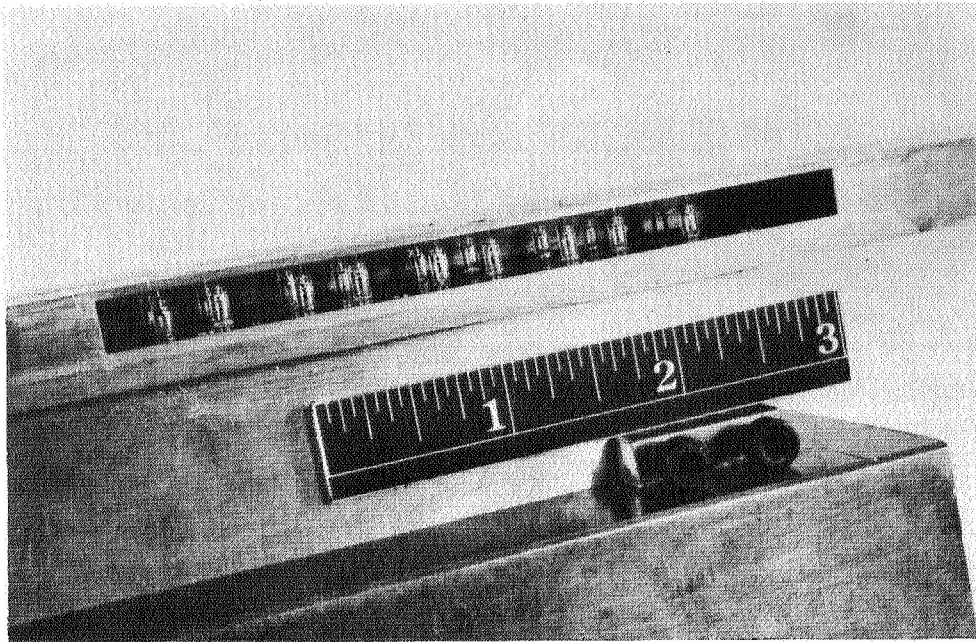
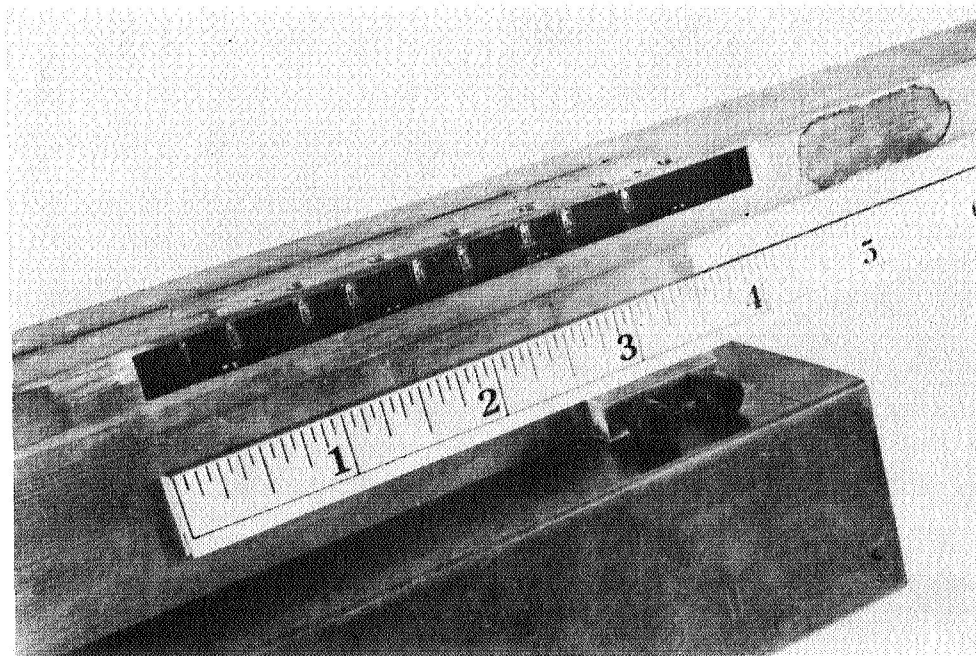


Figure 18. Diode and r-f choke holder.





(a)



(b)

Figure 19. Internal views of assembled array with one side-window removed.



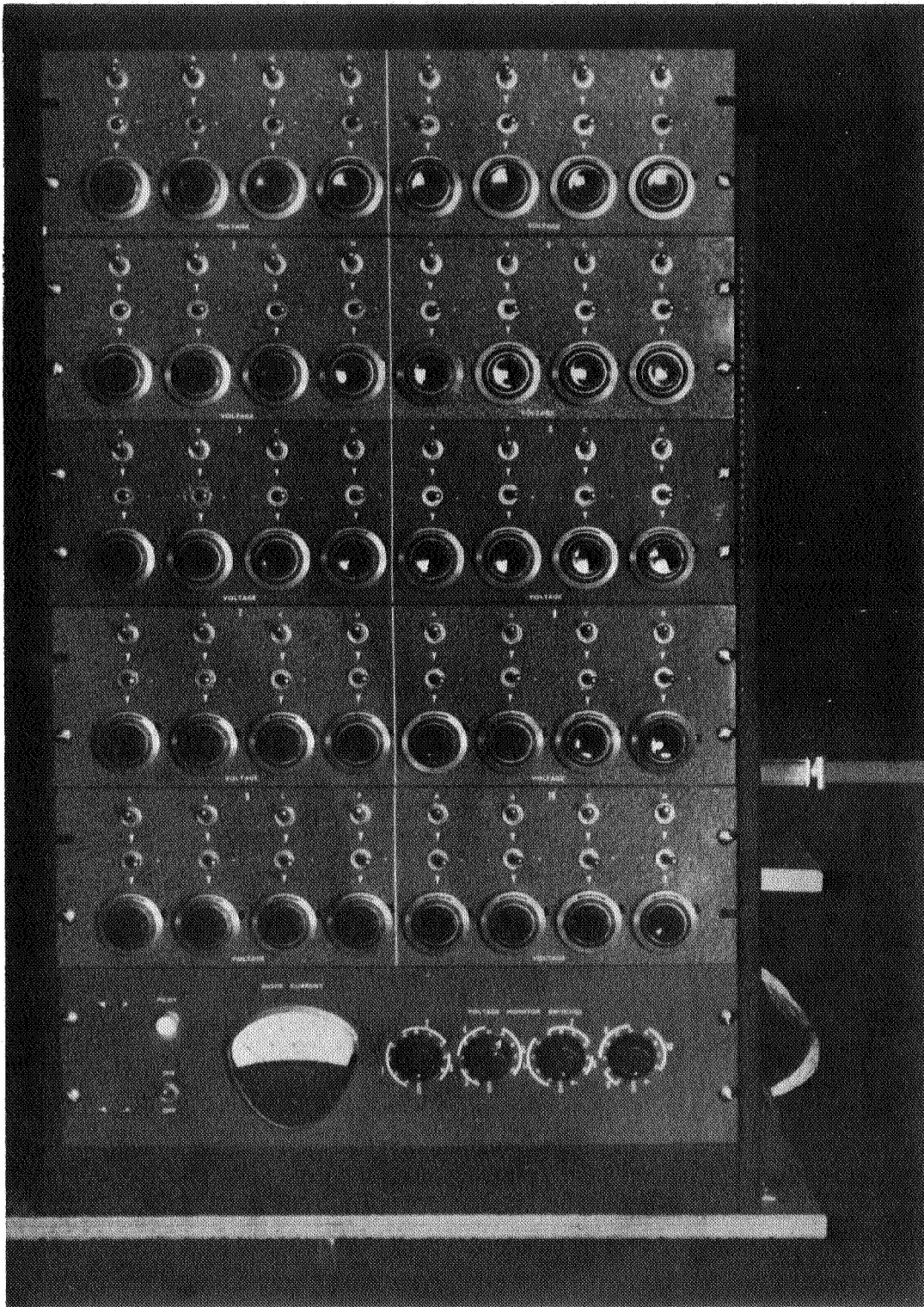


Figure 20. Diode-iris control panel for ten-element linear array.

$\pm 28.2$  degrees, and  $\pm 45$  degrees; and difference patterns at  $\theta = 0$  degree, and  $+45$  degrees. The necessary progressive phase shift  $\alpha$  along the array for a particular scan angle  $\theta$  was computed from the equation

$$\alpha = \pm \frac{2\pi d}{\lambda_0} \sin \theta = \pm 211^\circ \sin \theta$$

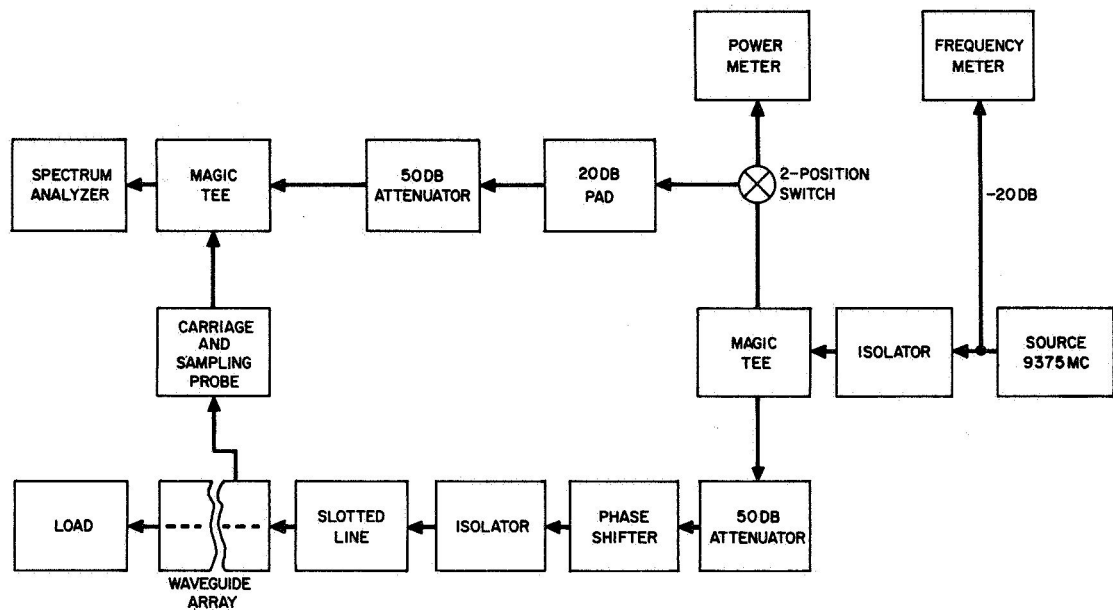
where

$\lambda_0$  = free space wavelength, and

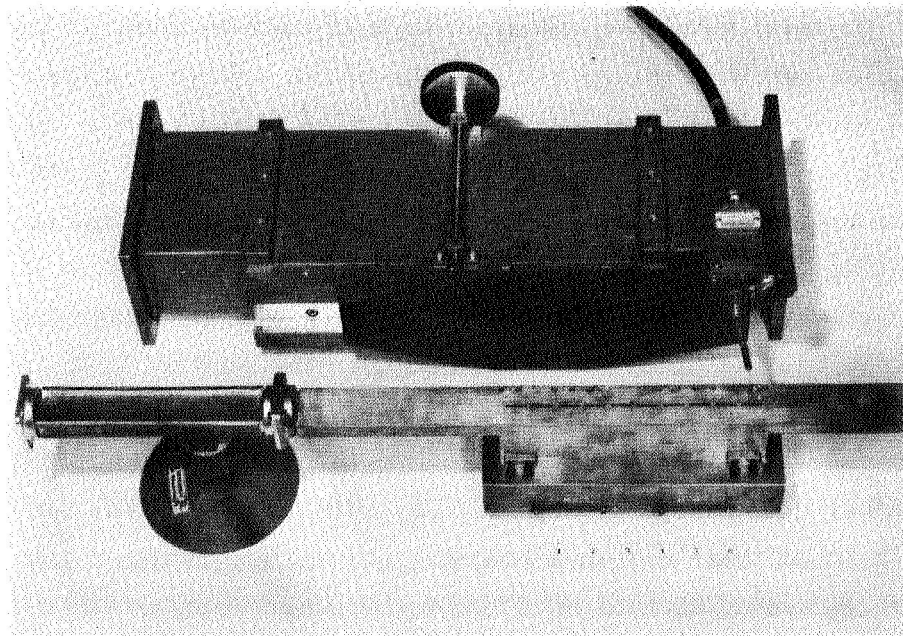
$d = 0.586 \lambda_0$  = element interspacing.

The seven aperture distributions were set up in the array with the aid of a microwave phase bridge circuit. The bridge circuit utilizes a radiation sampling probe, mounted on an accurately driven carriage, to obtain the relative phase and amplitude of each element in the aperture. A close view of this portion of the phase bridge is shown in Figure 21 along with a schematic of the entire phase bridge circuit.

The phase and amplitude of the element nearest the input to the array was established first and then followed by the relative excitation of succeeding elements. The desired coupling by each element was obtained by setting the precision phase shifter and attenuator in the bridge circuit to the desired values and then the control voltages of the four diodes associated with a given element were adjusted to reproduce these values. This procedure was followed for all slot radiators in the array. After completion of the coupling adjustment for the ten elements, it was found that their original coupling values had changed and that, in fact, four or five additional runs had to be made before satisfactory coupling values were obtained. The need for these readjustments suggests the presence of mutual coupling effects between slots; it is well to note that the technique in setting up the aperture distribution compensates for these mutual coupling effects.



(a) Schematic of entire circuit.



(b) Closeup of carriage and sampling probe.

Figure 21. Phase bridge circuit used for obtaining phase and amplitude distribution in linear array aperture.

Patterns and Gain Measurements. After recording the diode voltages needed to generate the seven aperture distributions, the linear array and associated control panel were moved and mounted on the turntable in the Hughes Anechoic chamber; in addition, ground planes were attached to the linear array as shown in Figures 22 and 23. The diode voltages were then reproduced for each distribution, and patterns and gain measurements were taken. Figure 24 shows a composite grouping of the five sum patterns that were taken at 9.375 Kmc. This figure clearly demonstrates the feasibility of the diode-iris technique to electronically scan the main beam of the linear array  $\pm 45$  degrees about the array normal; also, all beam pointing directions were accurate to within one degree of theoretical prediction. In addition to the sum patterns at  $\theta = 0, +45$  degrees, difference patterns were also recorded. These measured patterns are compared with their predicted patterns in Figure 25. The predicted patterns were calculated using the amplitude and phase values of each element obtained on the phase bridge circuit; these excitations were then programmed into a computer and the patterns calculated. As shown, good agreement between prediction and measurement was realized. These results are indicative of the accuracy achieved in controlling the phase progression and amplitude distribution in the aperture. The high sidelobe seen in the sum patterns for  $\theta = \pm 45$  degrees are second order beams due to the position of the scanned beam and the spacing between slot radiators. These beams are predicted by the theory and are not a limitation of the technique.

For the broadside pattern, the antenna gain was computed to be 13.2 db. The measured gain for the array was 5.7 db. The power delivered to the load and the reflection loss account for 0.75 db of this gain difference; the loss attributed to the ten diode-iris devices is 6.75 db or about 0.68 db per unit which agrees with that anticipated. Other pertinent characteristics of the array performance are given in Table 2.

Table 2. Performance of a diode-iris controlled linear array of ten elements with interelement spacing of  $0.586 \lambda_0$  at 9.375 Kmc.

Scan Angle $\theta$ (Degrees)		Pattern Type	Uniform Progressive Phase Shift (degrees)	Highest Measured Sidelobe (db)	Null-Depth of Measured Difference Pattern (db)	Antenna Input VSWR	Relative Power Into Load (percent)	Theoretical Antenna Gain (db)	Measured Antenna Gain (db)	Antenna Efficiency (percent)
Theoretical	Measured									
0.0	0.5	Sum	0	15.0	- - -	1.24	14.1	13.2	5.7	17.8
0.0	0.0	Difference	0	8.5	>26	1.14	14.0	- - -	- - -	- - -
28.2	28.0	Sum	-100	14.5	- - -	1.27	17.4	- - -	2.7	- - -
-28.2	-27.0	Sum	+100	14.5	- - -	1.55	12.9	- - -	- - -	- - -
45.0	43.5	Sum	-149	14.0*	- - -	1.28	17.8	- - -	3.1	- - -
45.0	47.0	Difference	-149	10.0	10.0	1.31	15.8	- - -	- - -	- - -
-45.0	-44.0	Sum	+149	14.0**	- - -	1.58	15.3	- - -	- - -	- - -

\*A second order beam appeared at about  $\theta = -70$  degrees which was 9 db down.

\*\*A second order beam appeared at about  $\theta = +68$  degrees which was 8 db down.

†The elements were not adjusted to radiate maximally.

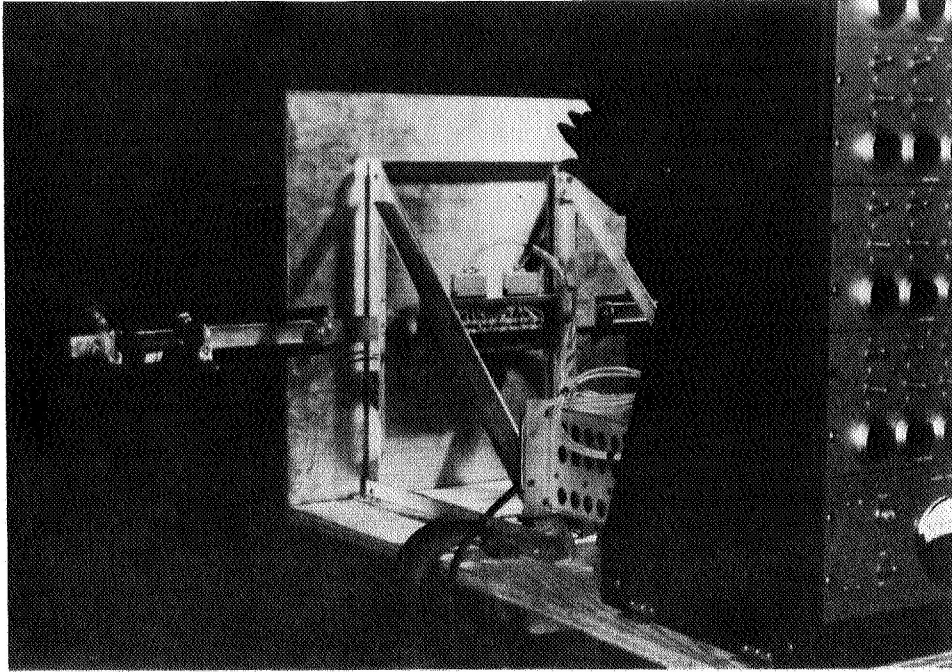


Figure 22. Rear view of linear array and control panel mounted on turntable.

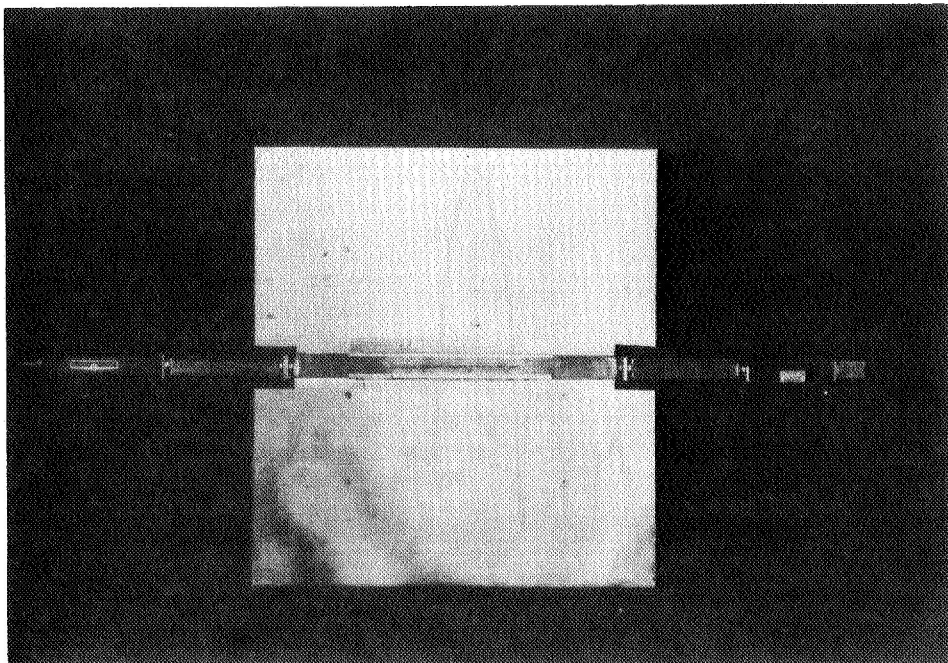
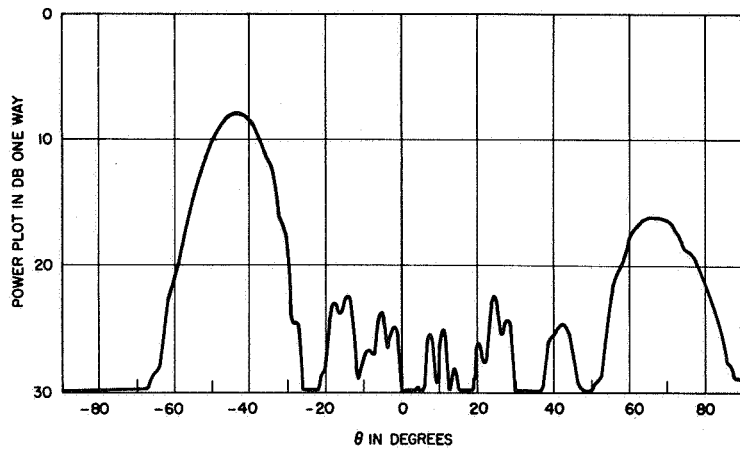
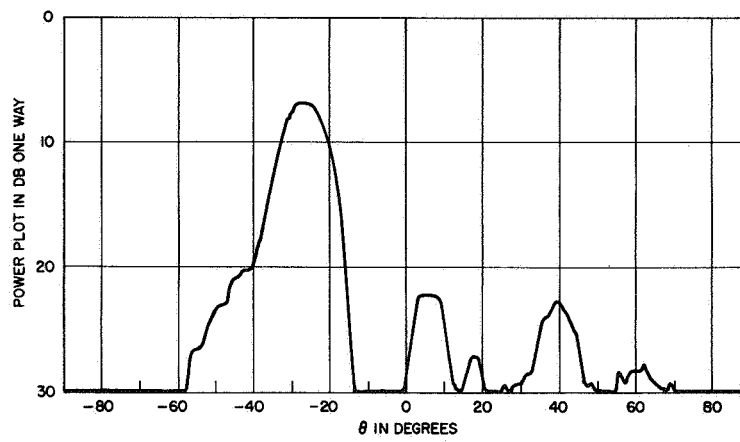


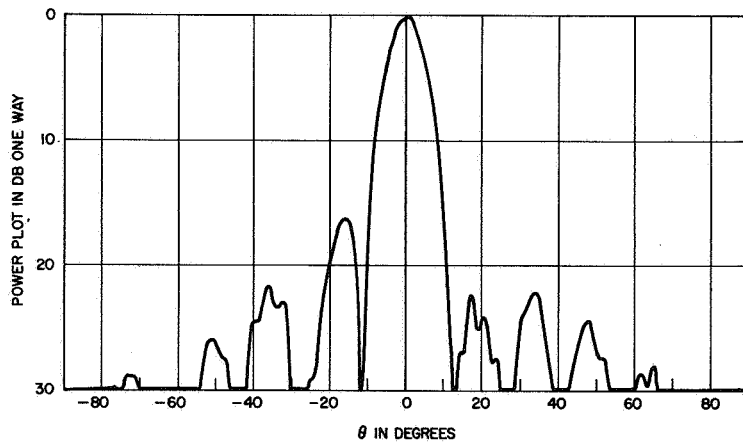
Figure 23. Front view of linear array in ground plane and mounted on turntable.



(a)  $\theta = -45^\circ$



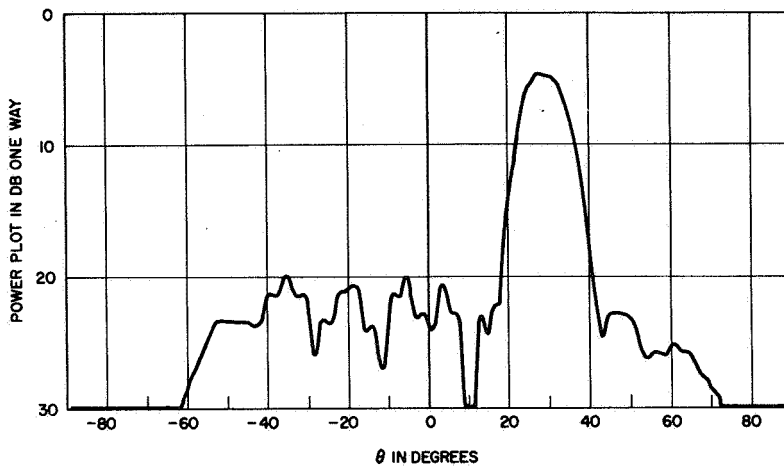
(b)  $\theta = -28.2^\circ$



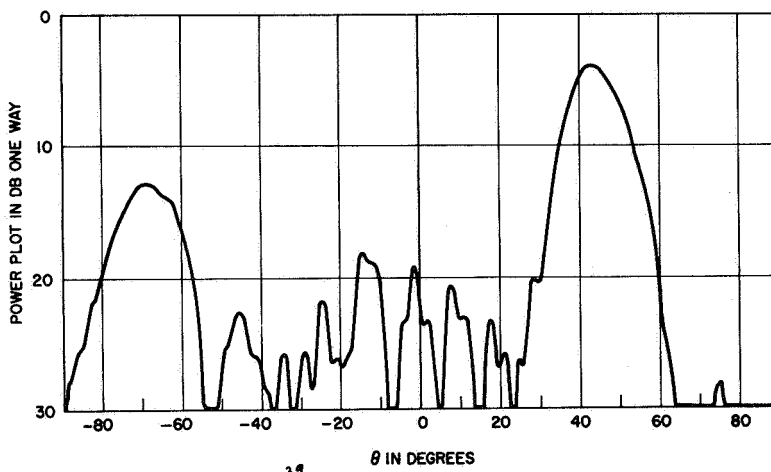
(c)  $\theta = 0^\circ$

Figure 24. Measured sum patterns illustrating 90 degrees of electronic beam scanning.



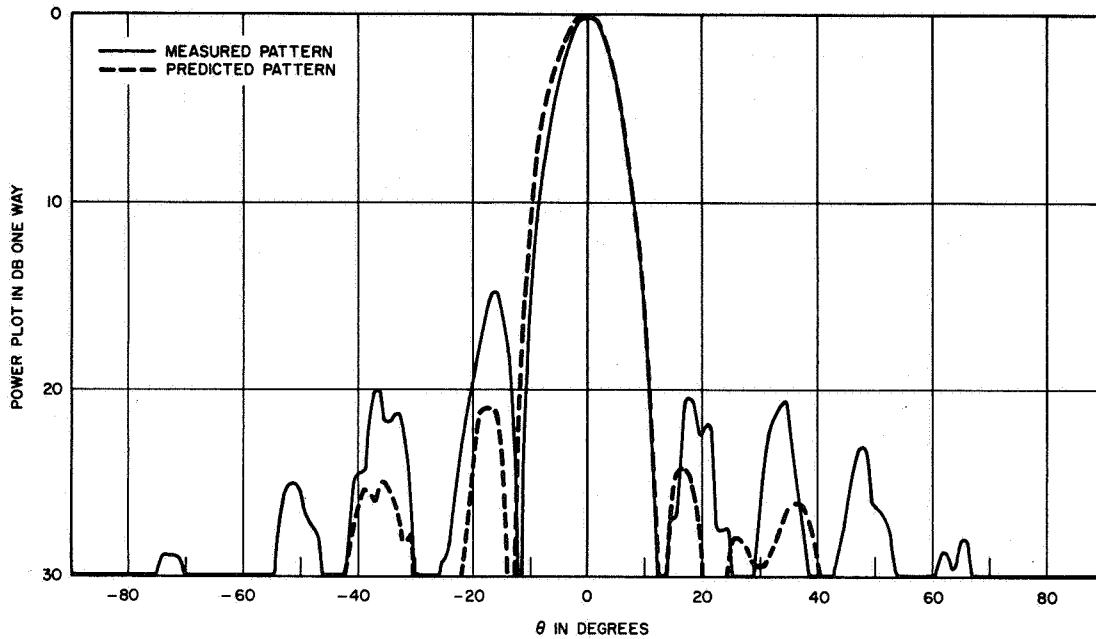


(d)  $\theta = +28.2^\circ$

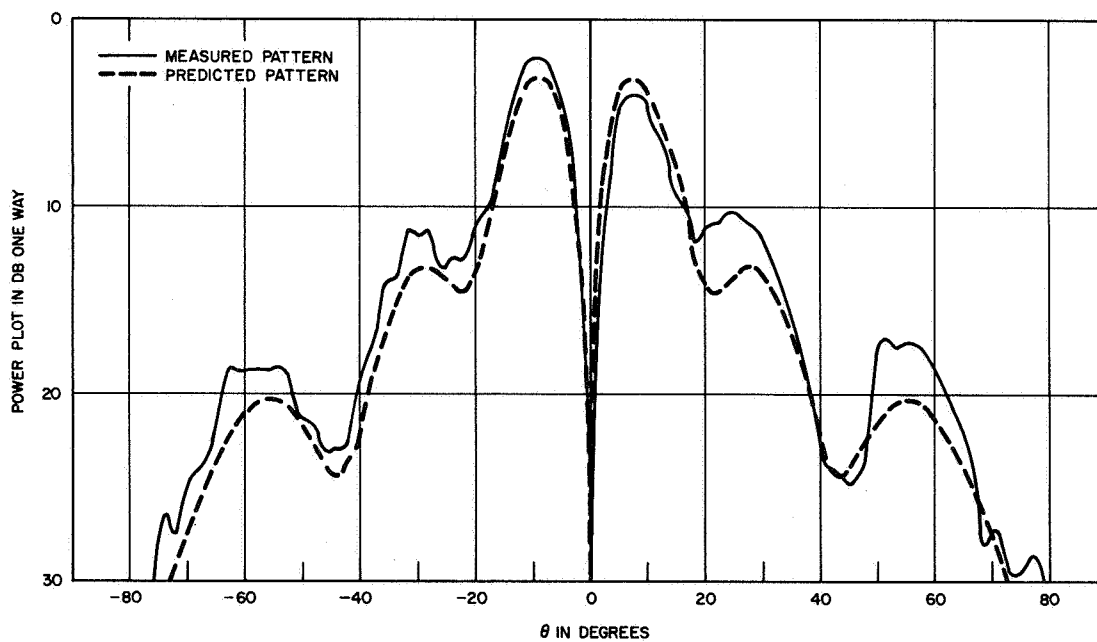


(e)  $\theta = +45^\circ$

Figure 24. Measured sum patterns illustrating 90 degrees of electronic beam scanning. (Continued)

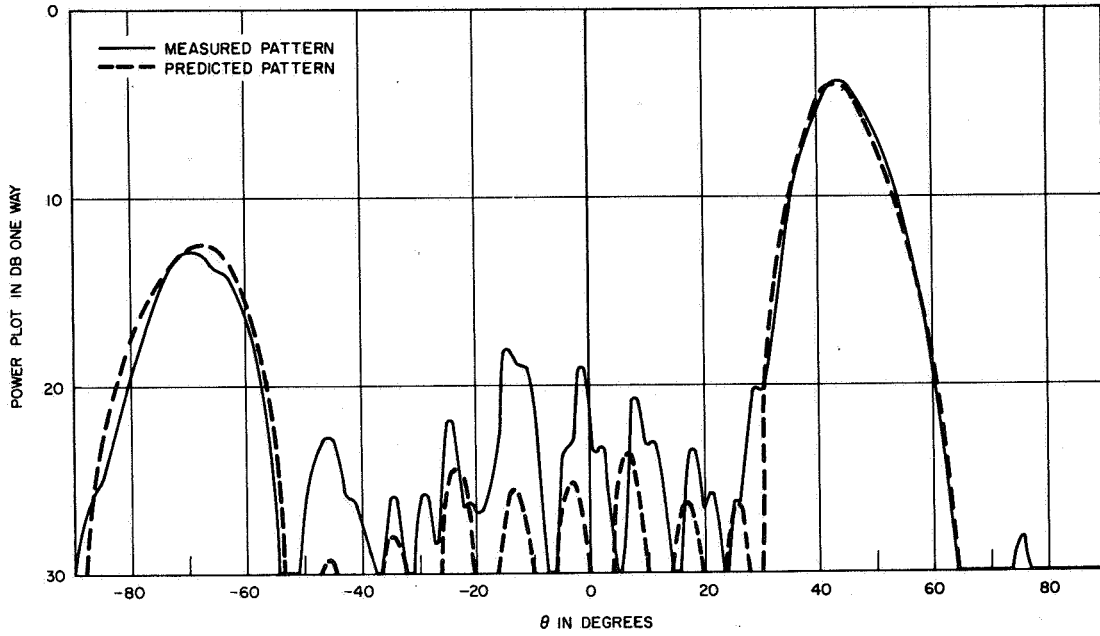


(a) Sum pattern at  $\theta = 0^\circ$

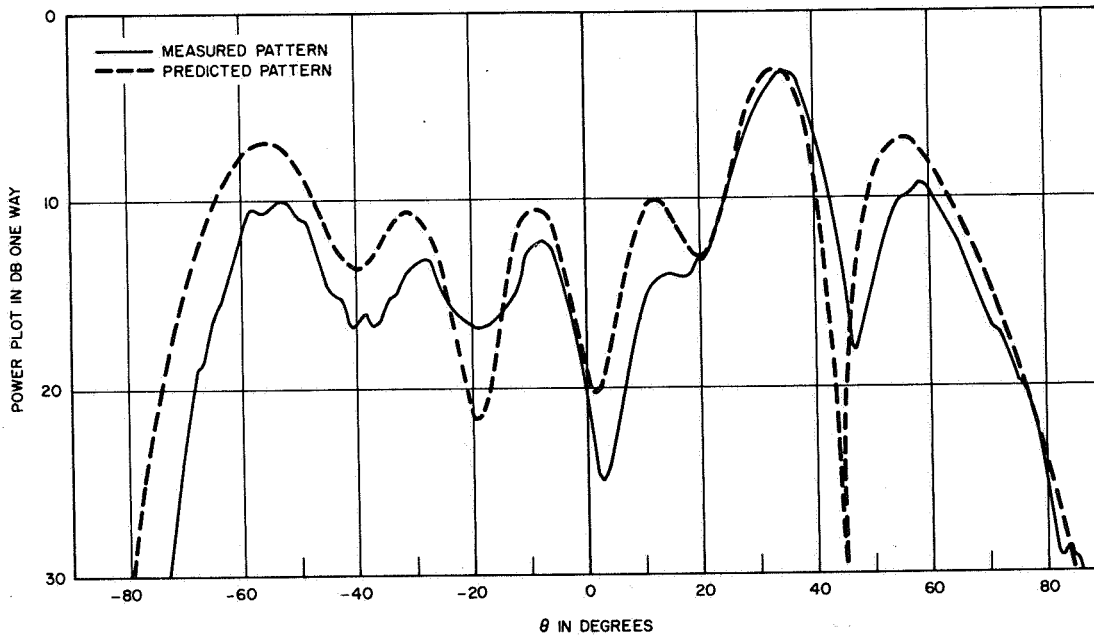


(b) Difference pattern at  $\theta = 0^\circ$

Figure 25. Comparison of predicted and measured sum and difference patterns for selected scan angles,  $\theta = 0$  degree and  $+45$  degrees.



(c) Sum pattern at  $\theta = +45^\circ$



(d) Difference pattern at  $\theta = +45^\circ$

Figure 25. Comparison of predicted and measured sum and difference patterns for selected scan angles,  $\theta = 0$  degree and  $+45$  degrees. (Continued)

#### D. REFERENCES

1. R. Tang, "A Slot with Variable Coupling and Its Application to a Linear Array," RLM (M)S6-15, Hughes Aircraft Company, July 1956.
2. B. J. Maxum, "Resonant Slots with Independent Control of Amplitude and Phase," TM No. 573, Hughes Aircraft Company, December 1957.
3. H. E. Shanks and V. Galindo, "Ferrite Excited Slots with Controllable Amplitude and Phase," TM No. 585, Hughes Aircraft Company, January 1960.
4. Norman Houlding, "Measurement of Varactor Quality," Microwave Journal, Vol. 3, No. 1, pp. 40-45, January 1960.
5. A. Uhler, Jr., "The Potential of Semiconductor Diodes in High Frequency Communications," Proc. IRE, Vol. 46, pp. 1099-1115, June 1958.

#### IV. CONCLUSIONS

This report summarized the results of a study of present and future manned-spacecraft missions which require rendezvous and lunar landing radar systems. The results contain a delineation of the requirements to be met by antenna systems for lunar rendezvous, lunar landing, and earth rendezvous mission segments. In addition, promising antenna techniques, whose development can be expected to provide enhanced mission performance and flexibility, were described in detail.

One such technique which employs a four-diode-iris configuration about a slot in a waveguide, was investigated and shown to provide accurate phase and amplitude control over the radiated field from the slot. A 10-element linear array which utilizes this technique, was designed and tested and shown to provide electronic beam scanning over a  $\pm 45$  degree interval about broadside. The measured sum and difference patterns were in good agreement with the predicted results. The gain of the array agreed with that anticipated.



## V. RECOMMENDATIONS

The experimental results achieved to date with the diode-iris controlled array suggests that further development work be done to explore and optimize the capability of the technique. Areas where further effort is required are:

1. Improvements in the insertion loss and coupling of the diode-iris device and linear array.
2. Investigations into r-f bandwidth capability of the device.
3. Studies of arbitrary pattern synthesis or beam shaping capability of the diode-iris controlled array.
4. Design of circuitry to dynamically demonstrate beam scanning with the array.

### 1. Insertion Loss and Coupling

Alternate schemes for feeding the elements in a slot array which improve the array efficiency by reducing the effect of the diode-iris insertion loss should also be considered. For example, by dividing the aperture of the linear array into two sections and feeding each section in parallel, the reduction in antenna efficiency, which is caused by the diode-iris insertion loss, can be reduced by a factor of about two. This feeding technique can be implemented by feeding the 10-element linear array at its center rather than at one end. This technique and its extension to additional array feed points can be considered in further investigations.

Further work should be done to optimize the coupling response and reduce the insertion loss of the diode-iris device. Optimization of coupling can be obtained by further refinements in the positioning of the diodes relative to the slot or by the use of varactor diodes with greater ranges in capacitance. A major reduction in the insertion loss of the iris must be one of the significant objectives of any further development effort.

The insertion loss is composed of both diode dissipation and reflection losses. Matching techniques have successfully reduced the



reflection loss of the 4-diode-iris control unit, but further refinement is always desirable. However, further reduction of the reflection loss over a useful range of amplitude and phase depends on a substantial lowering of the dissipative insertion loss. In connection with this problem, a study was made which correlated the device coupling and loss with the diode characteristics. It was found that the primary factor which governs the dissipative loss of the device is the diode series resistance and that lower values of this resistance result in lower dissipative loss. It was also determined that a low diode capacitance is required to obtain a large range of coupling control. Thus, experimentation with high-Q diodes that have lower series resistance and lower capacitance values should improve the performance of the iris-controlled device.\*

In connection with improved diode performance, attention must also be directed toward the power handling capability of diodes. The diodes that have been used in the X-band iris-control devices discussed in this report operate at low r-f powers (on the order of several hundred microwatts average power) and hence would only have application in passive or semi-active antenna systems. For active antennas or radar applications higher-power handling diodes are required. Presently, diodes are available which have been operated at several kilowatts peak power at frequencies through S-band.\*\* They require driving voltages on the order of several hundred volts and draw several amperes of current in the forward bias direction. The availability of these diodes suggests that they can be used in an iris-control device in which high-power requirements are to be satisfied.

The devices described so far were all designed for X-band. Because the Q values for the diodes used in these devices increase directly with wavelength, these same diodes should provide greater slot control

---

\*The Hughes Semiconductor Division, Costa Mesa, California, consulted on and provided diodes for the program.

\*\*Private communication from R. Tang, Ground Systems Division, Hughes Aircraft Company, Fullerton, California.

and lower dissipative insertion loss at C-band and S-band frequencies. Investigations at lower frequency should therefore result in considerable improvement in the microwave performance of the diode-iris control device. Plans should be made for the designing of test units in these lower frequency bands using the X-band diodes.

## 2. R-F Bandwidth Studies

One desirable feature of an antenna technique is its ability to provide satisfactory performance over a significant r-f frequency range. To date, limited effort has been given to investigating this aspect of the device. Therefore a study of bandwidth of the diode-iris control device should also be conducted.

## 3. Arbitrary Pattern Synthesis

The diode-iris controlled slot array has demonstrated electronic scan of sum and difference patterns over a 90 degree angular sector in space. Although these results illustrate the monopulse and scanning capability of the technique they do not reveal its overall versatility. Because the diode-iris device provides accurate control over both the amplitude and phase of the individual slot radiators, arbitrary pattern synthesis or beam shaping can be readily achieved; e. g. , the array aperture distribution might be adjusted to generate a radiation pattern with a cosecant-squared  $\theta$  dependence; this pattern shape has use in ground mapping and surveillance operations. The array can also generate a variety of sector beams or, in general, patterns which optimize the antenna performance relative to a given function and operating environment. This pattern versatility is one feature of the diode-iris control device which should be explored and illustrated in further development efforts.

## 4. Dynamic Beam Scanning

Finally, the array patterns shown in this report are generated by manually adjusting the driving voltages associated with each diode.

To implement the scan capability associated with this technique, the design and testing of control circuits which dynamically move a beam in space should also be considered.

*"The aeronautical and space activities of the United States shall be conducted so as to contribute . . . to the expansion of human knowledge of phenomena in the atmosphere and space. The Administration shall provide for the widest practicable and appropriate dissemination of information concerning its activities and the results thereof."*

—NATIONAL AERONAUTICS AND SPACE ACT OF 1958

## NASA SCIENTIFIC AND TECHNICAL PUBLICATIONS

**TECHNICAL REPORTS:** Scientific and technical information considered important, complete, and a lasting contribution to existing knowledge.

**TECHNICAL NOTES:** Information less broad in scope but nevertheless of importance as a contribution to existing knowledge.

**TECHNICAL MEMORANDUMS:** Information receiving limited distribution because of preliminary data, security classification, or other reasons.

**CONTRACTOR REPORTS:** Scientific and technical information generated under a NASA contract or grant and considered an important contribution to existing knowledge.

**TECHNICAL TRANSLATIONS:** Information published in a foreign language considered to merit NASA distribution in English.

**SPECIAL PUBLICATIONS:** Information derived from or of value to NASA activities. Publications include conference proceedings, monographs, data compilations, handbooks, sourcebooks, and special bibliographies.

**TECHNOLOGY UTILIZATION PUBLICATIONS:** Information on technology used by NASA that may be of particular interest in commercial and other non-aerospace applications. Publications include Tech Briefs, Technology Utilization Reports and Notes, and Technology Surveys.

*Details on the availability of these publications may be obtained from:*

SCIENTIFIC AND TECHNICAL INFORMATION DIVISION  
NATIONAL AERONAUTICS AND SPACE ADMINISTRATION

Washington, D.C. 20546